Recent decadal trends in global phytoplankton composition

Cecile S. Rousseaux [1,2,*] and Watson W. Gregg [1]

[1] Global Modeling and Assimilation Office, NASA Goddard Space Flight Center, Greenbelt, Maryland, USA

[2] Universities Space Research Association, Columbia, Maryland, USA

***** Author to whom correspondence should be addressed; E-Mail: Cecile.S.Rousseaux@nasa.gov;
Tel.: +1-301-614-5750; Fax: +1-301-614-5644

Abstract

Identifying major trends in biogeochemical composition of the oceans is essential to improve our understanding of biological responses to climate forcing. Using the NASA Ocean Biogeochemical Model (NOBM) combined with ocean color remote sensing data assimilation, we assessed the trends in phytoplankton composition (diatoms, cyanobacteria, coccolithophores and chlorophytes) at a global scale for the period 1998-2012. We related these trends in phytoplankton to physical conditions (surface temperature, surface photosynthetically available radiation [PAR] and mixed layer depth [MLD]) and nutrients (iron, silicate and nitrate). We found a significant global decline in diatoms (-1.22% y^{-1}, $P<0.05$). This trend was associated with a significant ($P<0.05$) shallowing of the MLD (-0.20% y^{-1}), a significant increase in PAR (0.09% y^{-1}) and a significant decline in nitrate (-0.38% y^{-1}). The global decline in diatoms was mostly attributed to their decline in the North Pacific (-1.00% y^{-1}, $P<0.05$) where the MLD shallowed significantly and resulted in a decline in all three nutrients ($P<0.05$). None of the other phytoplankton groups exhibited a significant change globally, but regionally there were considerable significant trends. A decline in nutrients in the northernmost

latitudes coincided with a significant decline in diatoms (North Pacific, -1.00% y^{-1}) and chlorophytes (North Atlantic, -9.70% y^{-1}). In the northern mid-latitudes (North Central Pacific and Atlantic) where nutrients were more scarce, a decline in nutrients was associated with a decline in smaller phytoplankton: cyanobacteria declined significantly in the North Central Pacific (-0.72% y^{-1}) and Atlantic (-1.56% y^{-1}) and coccolithophores declined significantly in the North Central Atlantic (-2.06% y^{-1}). These trends represent the diversity and complexity of mechanisms that drives phytoplankton communities to adapt to variable conditions of nutrients, light, and mixed layer depth. These results provide a first insight into the existence of trends in phytoplankton composition over the maturing satellite ocean color era and illustrate how changes in the conditions of the oceans in the last ~15 years may have affected them.

Introduction

The effects of climate variability on the physics and biology of the oceans have become apparent in the last decades. Changes in ocean properties relevant to climate, e.g., increasing temperature, CO_2 (acidification) and sea level, have been observed during the past 40 years [*Stocker et al.*, 2013]. Many variables are not routinely measured and/or have only been measured for a relatively short time period, not enough to assess the existence of trends. Phytoplankton composition for example, although a key player in ocean biodiversity, the storage of CO_2 and the recruitment of higher trophic levels, remains spatially and temporally under-characterized. Satellites provide a tool allowing for the characterization of phytoplankton communities globally at a high temporal resolution. In recent years, approaches to derive phytoplankton composition from satellite ocean color have multiplied [e.g. *Alvain et al.*, 2005; *Ciotti et al.*, 2002; *Hirata et al.*, 2011; *Mouw and Yoder*, 2006; *Uitz et al.*, 2006]. These methods are often developed for a specific satellite application (SeaWiFS or MODIS) and may therefore be only applicable to a specific sensor (unless further validation is accomplished) thereby providing a maximum of ~12 years data.

Establishing the existence of trends requires long record [*Henson et al.*, 2010]. The existence of global ocean color coverage since the late 90s provides an opportunity for assessing the existence of trends in phytoplankton. The challenge has been to combine the different ocean color missions to produce a consistent time series that would allow the detection of such trends. Some authors have proposed solutions to provide a consistent ocean color times series across ocean color missions [i.e. *Antoine et al.*, 2005; *Gregg and Conkright*, 2002; *Gregg and Casey*, 2009; *Martinez et al.*, 2009]. Previous studies assessing the existence of trends in phytoplankton looked at chlorophyll and were mostly based on one ocean color sensor and reported no significant trend in chlorophyll in the global pelagic ocean, for example *Gregg et al.* [2005] for the period 1998-2003 and *Beaulieu et al.* [2013]

for the period 1998-2007. *Gregg and Rousseaux* [2014] found no significant change in the global pelagic ocean for a 15-year period, 1998-2012, using two bias-corrected and assimilated ocean color observational records. Some authors have also looked at in situ chlorophyll proxies over longer time scales to assess the presence of trends in total chlorophyll. *Boyce et al.* [2014] for example, using a database of historical measurements from 1890 to 2010, detected a significant decline in chlorophyll over 62% of the global ocean surface area where data were present. In another effort, *Wernand et al.* [2013] used the Forel-Ule scale record, a record based on a scale used to classify the color of open water, to report trends since 1889. Their analysis revealed no global trend during the past century but found some significant trends regionally.

While these efforts have provided a first line of information on the existence of trends in ocean biology, there remains very little known about the global and large scale regional trends in phytoplankton composition. Several studies highlighted regional trends in the phytoplankton communities. This includes the expansion of warm water species into intermediate waters in the North Atlantic [*Barnard et al.*, 2004; *Beaugrand et al.*, 2002] and the alteration of phytoplankton community structure in the Humboldt current, the north sea and the north east Atlantic [*Alheit and Niquen*, 2004; *Beaugrand*, 2004; *Richardson and Schoeman*, 2004]. Modeling studies [*Doney*, 2006] have suggested that climate change would lead to increasing stratification which would lead to lower nutrient levels in the tropics but more light available for photosynthesis in the high latitudes. The faster warming of the oceans in the northern hemisphere than in the southern hemisphere [*Flato and Boer*, 2001; *Gent and Danabasoglu*, 2011] could also lead to different trends in the phytoplankton composition. In this study we assess the trends in phytoplankton composition at a global scale for the period from 1998 until 2012 using multiple ocean color satellites and a numerical model to establish potential links between trends in phytoplankton composition and changes in physical and nutrient

conditions. Phytoplankton groups are quantitatively characterized in the underlying model based on interactions with the physical and biological environment and modified using assimilation of a consistent time series of satellite chlorophyll observations.

Material and Methods

The physical conditions (surface temperature and mixed layer depth [MLD]), nutrient concentrations (nitrate, silicate and iron) and phytoplankton composition (diatoms, cyanobacteria, coccolithophores and chlorophytes) are obtained from the NASA Ocean Biogeochemical Model (NOBM), a three dimensional biogeochemical model of the global ocean coupled with a circulation and radiative model [*Gregg and Casey*, 2007; *Gregg et al.*, 2003]. Surface photosynthetically available radiation [PAR] is derived from the Ocean-Atmosphere Spectral Irradiance Model [OASIM; *Gregg and Casey*, 2009]. NOBM has a near-global domain that spans from -84° to 72° latitude at a 1.25° resolution in water deeper than 200 m. NOBM is coupled with the Poseidon ocean general circulation model, which is driven by wind stress, sea surface temperature, and shortwave radiation.

The biological portion of the model contains 4 explicit phytoplankton taxonomic groups (diatoms, cyanobacteria, chlorophytes and coccolithophores), 3 detritus components (silicate, nitrate/carbon and iron), 4 nutrients (nitrate, silicate, iron and ammonium) and one zooplankton group. The phytoplankton groups differ in maximum growth rates, sinking rates, light and nutrient requirements, and optical properties [Gregg et al., 2013]. In the model, the diatoms and cyanobacteria represent functional extremes. The high growth rates of diatoms allow them to flourish in areas of abundant nutrients (high latitude, coastal and equatorial upwelling) but their large

sinking rate prevent them from dominating in quiescent regions. Cyanobacteria represent a combination of *Synechococcus*, *Prochlorococcus* as well as nitrogen fixers such as *Trichodesmium*. Cyanobacteria have a slow growth rate, but their high nitrogen uptake efficiency, slow sinking rate and ability to fix nitrogen allow them to sustain in low nitrogen areas (e.g. mid-ocean gyres). The chlorophytes represent an intermediate group, occupying the transitional regions between the high nutrients regions dominated by the larger diatoms and the nutrient-scarce regions dominated by cyanobacteria. Chlorophytes are intended to represent a multitude of phytoplankton species occupying these intermediate regions, including, but not limited to prasinophytes, prymnesiophytes, pelagophytes, cryptomonads, chlorophytes themselves, and other nano-eukaryotes. *Phaeocystis* spp. is a particularly important functional group represented poorly by chlorophytes in high latitudes since the growth of chlorophytes at those latitude is limited by temperature. The coccolithophores have an ability to tolerate lower nutrient conditions than diatoms and chlorophytes, but not as low as cyanobacteria, and have the property of sinking faster than most phytoplankton despite their small size. We recognize that this is an oversimplification of the natural ecosystems but models are limited by the availability of optical and physiological data on each of these phytoplankton groups to parameterize the model as well as computational cost. Carbon-to-chlorophyll ratios vary in the model as a function of light availability.

The growth of phytoplankton is dependent on total irradiance, nitrogen (nitrate+ammonium), silicate (for diatoms only), iron and temperature. The nutrient-dependent growth fractions are the same type for all the nutrients with different half saturation constant (for k_n, k_{Si} and k_{Fe}, see Table 1). For example, the nitrate-dependent growth fraction is:

$$\omega(NO_3)_i = \frac{NO_3}{NO_3 + (k_n)_i}$$

An additional adjustment to reduce the growth rate of cyanobacteria in cold water (<15°C) is made [*Gregg et al.*, 2003, based on Agawin et al., 1998, 2000 and Li et al., 1998]. The temperature dependence growth is directly from Eppley [1972] which produces a temperature-growth normalized to 20°C. The fraction of growth due to the irradiance is equal to the total irradiance divided by the sum of the total irradiance and the half-light saturation parameter [see *Gregg and Casey*, 2007; *Gregg et al.*, 2003].

Bias-correction of the satellite chlorophyll data is performed prior to assimilation using public in situ archives in the Empirical Satellite Radiance-In situ Data (ESRID) methodology [*Gregg et al.*, 2009]. This method uses relationships between satellite water-leaving radiances and in situ data (Sea-Viewing Wide Field-of-View Sensor (SeaWiFS) and Moderate Resolution Imaging Spectroradiometer (MODIS) Aqua-Level 3) to improve estimates of surface variables while relaxing requirements on post-launch radiometric re-calibration [*Gregg et al.*, 2009]. To this end, we use the latest satellite data produced by NASA and global in situ fluorometric chlorophyll data collected from the National Oceanographic Data Center [NODC; *Gregg and Conkright*, 2002], NASA in situ [*Werdell and Bailey*, 2005], and Atlantic Meridional transect [*Aiken and Bale*, 2000] archives [*Gregg et al.*, 2009]. The application of ESRID reduces the bias of SeaWiFS (as compared to in situ data) from 13.8% to -4.7% and MODIS-Aqua from 5.9% to -1.4% [*Gregg and Rousseaux*, 2014]. The time series uses data from SeaWiFS for 1998-2002, then switches to MODIS-Aqua data. The ESRID method has the attribute of reducing discontinuities between the two satellite data sets [*Gregg and Casey*, 2010], enabling the construction of a consistent 15-year time series of global ocean chlorophyll. Gregg and Rousseaux [2014] showed that discontinuities in global median chlorophyll were eliminated and trend statistics for the combined SeaWiFS-MODIS time series were statistically indistinguishable from the trends of each mission time series independently. In contrast,

the combined time series without ESRID correction exhibited an anomalous significant decline in global median chlorophyll, due to the inconsistencies between sensors [*Gregg and Rousseaux*, 2014].

The model is spun up in free-run mode for 35 years using climatological forcing from Modern-Era Retrospective analysis for Research and Applications [MERRA; *Rienecker et al.*, 2011]. An additional 65 years assimilating climatological ESRID-MODIS chlorophyll is used to find a 15-year segment with the smallest model drift in global nutrients. Although satisfactory for the analysis of total chlorophyll [*Gregg and Rousseaux*, 2014], residual model drift in nutrients continues to slightly affect distributions of phytoplankton groups in the small basins of the Equatorial and North Indian. Consequently, the model is integrated an additional 100 years, and the smallest 15-year drift is chosen from this extended run. The lowest absolute drift in nutrients is 0.02% y^{-1} for the 15 years beginning in simulation year 2120. The conditions corresponding to this simulation year are then used to start the transient run in September 1997 using transient atmospheric monthly forcing.

Bias-corrected SeaWiFS and MODIS-Aqua chlorophyll data (using ESRID) are assimilated daily. ESRID-SeaWiFS is used for the period 1998-2002, and ESRID-MODIS-Aqua from 2003 to 2012. Phytoplankton groups are not directly assimilated. Their relative abundances are kept constant in the total chlorophyll assimilation [*Gregg*, 2008]. Nutrients are adjusted corresponding to the chlorophyll assimilation using nutrient-to-chlorophyll ratios embedded in the model [*Rousseaux and Gregg*, 2012]. However, phytoplankton relative abundances respond to changes in the physical environment (e.g., light penetration, nutrient availability, horizontal and vertical gradients) that are affected by the assimilation of total satellite chlorophyll. The concentrations reported in this paper are representative of the first layer of the MLD.

The trends are calculated by fitting a least-square linear regression and calculating the corresponding p-value and correlation coefficient. A statistical trend is defined as one with a p-value smaller than 0.05. The trends are calculated using area weighted annual mean or median (mean for physical conditions and nutrients; median for phytoplankton groups and total chlorophyll). Using the autocorrelation function described in Box et al. [1994] we ruled out the existence of autocorrelation in the time series residuals.

Phytoplankton composition is validated using a publicly available database (http://gmao.gsfc.nasa.gov/research/oceanbiology/data.php). Global phytoplankton composition from the NOBM is within 20% of the in situ database for diatoms (18.2%, model higher than in situ data) and chlorophytes (-17.4%) and within 2-3% for cyanobacteria (1.3%) and coccolithophores (-2.8%). Global model nitrate comparison with National Oceanographic Data Center climatologies [*Conkright et al.*, 2002] are within 2.8% and silicate within -16%. Model dissolved iron compares within 13.6% of an in situ data set, available at the same location as phytoplankton data.

Results

At a global scale, annual median diatom concentrations declined significantly (0.006 µg chl L^{-1} or -1.22% y^{-1}, Tables 2 & 3) between 1998 and 2012 (Table 2). This decline in diatoms was associated with a significant shallowing of the MLD of ~1.8m between 1998 and 2012 (-0.20% y^{-1}), an increase in PAR (0.46 moles quanta m^{-2} d^{-1} or 0.09% y^{-1}) and a decline in nitrate (-0.32 µmol L^{-1} or -0.38% y^{-1}) (Figure 1 & Tables 2 & 3). Of the 12 major oceanographic regions, diatom concentrations declined significantly in three regions (North Pacific, North Indian and Equatorial Indian, Table 2). In the North Pacific, there was a significant shallowing of the MLD (-1.00% y^{-1}, Figure 2) that coincided with a significant decline in all three nutrients (between -1.10% y^{-1} for

nitrate and -0.79% y^{-1} for silicate) and a significant increase in PAR (0.21% y^{-1}, Figure 3). The significant decline in nutrients resulted in a decline in diatoms (-1.00% y^{-1}) and total chlorophyll (-1.07% y^{-1}). Note that the distribution and trends in silicate were very similar to those of nitrate and therefore we do not include a figure of the distribution and trends for this nutrient.

While in the North Pacific the significant shallowing of the MLD was likely the cause of the decline in all nutrients and diatoms, the situation in the North and Equatorial Indian, the two other regions with a significant decline in diatoms, was more complex. In the North Indian Ocean there was a significant deepening of the MLD (0.50% y^{-1}) associated with a significant increase in iron (1.47% y^{-1}, Figure 4) and significant decline in nitrate (-2.87% y^{-1}, Figure 5). There was a shift in the phytoplankton composition characterized by a significant decline in diatoms (-5.89% y^{-1}), chlorophytes (-2.73% y^{-1}), total chlorophyll (-2.41% y^{-1}) and a significant increase in cyanobacteria (9.83% y^{-1}). The deepening of the MLD was mostly located in the Arabian Sea (Figure 6) and although significant, the deepening of 0.50% y^{-1} only represented a deepening of the MLD of ~2m between 1998 and 2012. In the Equatorial Indian, the situation was very similar to that in the North Indian. There was a phytoplankton composition shift with a significant decline in diatoms (-2.22% y^{-1}), chlorophytes (-6.02% y^{-1}) and total chlorophyll (-1.21% y^{-1}) and significant increase in cyanobacteria (2.64% y^{-1}). In the Equatorial Indian however, the significant decline in nitrate (-4.95% y^{-1}) and increase in iron (1.10% y^{-1}) occurred without any significant trend in the MLD.

Although there were only three regions where significant trends in diatoms were found, there were other regions such as the Southern Ocean and North Atlantic where despite the lack of statistically significant trends, there was a noticeable decline in diatoms in portions of these regions. In the Southern Ocean (defined as south of 40°S) for example, diatoms declined throughout most of the regions south of 60°S (except in the Weddell Sea where an increase in diatoms occurred).

Between 40°S and 60°S however, there were several areas of considerable increase in diatoms. For example, off the Patagonian shelf and south east of Australia there was a noticeable increase in diatoms that coincided with a deepening of the MLD, an increase in PAR and an increase in nitrate.

In the Pacific and Atlantic Ocean, there was a strong north-south gradient in the trends. In the northernmost latitudes, there was a significant decline in phytoplankton while in the regions south of 10°N there were only positive trends and these were always associated with nutrients and/or PAR (except for coccolithophores in the Equatorial Pacific). In the regions north of 40°N, a significant decline in all nutrients (except for silicate in the North Atlantic) resulted in a significant decline in diatoms (-1.00 % y^{-1}) in the North Pacific and chlorophytes (-9.70% y^{-1}) in the North Atlantic. In the North Pacific, the decline in all three nutrients was associated with a shallowing of the MLD (-1.00% y^{-1}, Figure 2) and a significant increase in PAR (0.21% y^{-1}, Figure 3). In the North Atlantic, there was a shift in phytoplankton composition with a significant decline in chlorophytes (-9.70% y^{-1}) and an increase in coccolithophores (5.96% y^{-1}) that coincided with a significant decline in nitrate (-0.88% y^{-1}) and iron (-1.79% y^{-1}). Although the spatially averaged trend in diatoms in the North Atlantic was not significant, there was a clear decline in diatoms between 45°N and 60°N that coincided with a decline in nitrate and iron (Figure 5 & Figure 7). The spatially-averaged significant increase in coccolithophores was due to a local increase in their abundance in the waters directly off the western European Shelf (Figure 7).

In the northern mid-latitudes (North Central Pacific and Atlantic), cyanobacteria (and coccolithophores in the North Central Atlantic) declined significantly (Tables 2 & 3, Figure 8 & Figure 9). Similarly to the North Pacific, the MLD shallowed in the North Central Pacific (-0.43% y^{-1}) and was associated with a significant increase in PAR (0.08% y^{-1}) and a significant decline in

nitrate (-2.70% y^{-1}) and total chlorophyll (-1.05% y^{-1}). Iron also declined significantly in the North Central Atlantic (-1.19% y^{-1}) and silicate (-1.87% y^{-1}) in the North Central Pacific.

South of 10°S, PAR increased significantly in all regions of the Atlantic and Pacific (Tables 2 & 3). The significant increase in PAR in the South Pacific (0.09% y^{-1}) was mostly in the area directly off the western side of South America (Figure 3). Note that despite a relatively large area off north-east Australia where PAR declined considerably, the spatially-averaged trend remained significantly positive. Silicate increased significantly in the Equatorial Atlantic (3.97% y^{-1}) and PAR increased significantly in the South Atlantic (0.09% y^{-1}). In the Equatorial Atlantic, the highest increase in silicate concentration was found along the coast and into the equatorial waters (data not shown). Directly south of that area, PAR increased by ~2.5 moles quanta m^{-2} d^{-1} (Figure 3), which was most likely responsible for making the spatially-averaged trend for the South Atlantic positive.

Finally in the Southern Ocean, there was a significant increase in silicate (0.23% y^{-1}), nitrate (0.13% y^{-1}) and PAR (0.20% y^{-1}) (Tables 2 & 3). There was not a consistent increase in any of these variables throughout the Southern Ocean. Instead, some areas such as the Bellingshausen Sea and the Amundsen Sea had a strong increase in nitrate and silicate (both nutrients had similar trend distribution) while other areas, directly south of the Indian Ocean for example, were experiencing a decline in those nutrients (Figure 5). The significant increase in the spatially-averaged PAR was the result of an increase along 40°S (Figure 3). South of this latitude, PAR was, although not significantly, mostly declining.

Discussion

Our results indicate that there is a global decline in diatoms that can be mostly attributed to a decline in the northern high latitudes of the Pacific Ocean and results from a decline in nutrients,

which, in turn derive from a shallowing MLD. Although not significant in the basin median, there are also large areas of significant diatom declines in the North Atlantic, up to 20%, also driven by significantly reduced nutrients (Figure 6 and Figure 5, respectively). The diatom decline does not lead to any phytoplankton shifts in the North Pacific, but in the North Atlantic, coccolithophores significantly increase and expand westward into regions previously occupied by diatoms and chlorophytes. While nutrients decline in the Pacific and Atlantic regions north of 10°N, the phytoplankton groups affected by this change differ. In the high latitudes where MLD temperature and light can limit groups like cyanobacteria, the decline in nutrients is detrimental to diatoms, which are the predominant group here. In the northern mid-latitudes (North Central Pacific and Atlantic), the decline in nutrients leads to a decline in smaller phytoplankton instead (i.e. cyanobacteria and coccolithophores). This suggests that the nutrient concentrations in this region are so low that even the cyanobacteria, which are characterized by very low nutrient requirement, are negatively impacted by it. This challenges the paradigm that increasing warming and therefore stratification would give an advantage to smaller phytoplankton [e.g. *Behrenfeld et al.*, 2006; *Polovina et al.*, 2008; *Steinacher et al.*, 2010]. The data suggest that the increasing stratification leads to nutrient levels that negatively impact all phytoplankton groups.

The vast majority of studies on changes in phytoplankton have focused on trends in total chlorophyll [e.g. *Agirbas et al.*, 2015; *Gregg and Rousseaux*, 2014; *Henson et al.*, 2010], climate variability [e.g. *Hays et al.*, 2005; *Masotti et al.*, 2011; *Polovina and Woodworth*, 2012; *Rousseaux and Gregg*, 2012] and changes in phenology [e.g. *Hashioka et al.*, 2013; *Racault et al.*, 2012; *Treusch et al.*, 2012]. The analysis of trends requires a relatively long time series and therefore the existence of studies on trends in phytoplankton composition remain to this date relatively scarce. A few modeling studies assessing the potential effect of climate change, including increasing

stratification and CO_2, have proposed that diatoms would decrease at high latitudes [*Bopp et al.*, 2005; *Boyd and Doney*, 2002; Table 3]. Declining diatom/microphytoplankton populations in the North Atlantic has been observed previously [e.g. *Agirbas et al.*, 2015; *Lomas et al.*, 2010; Table 3] although some studies also reported increasing diatom abundance in localized regions of the North Atlantic [i.e. *Hinder et al.*, 2012]. Our results show no basin-wide change in diatoms, but there are sizeable portions where they decline (Figure 6). Trends in smaller phytoplankton are more mixed. While we observe significant declining trends in cyanobacteria in the North Central Atlantic [similarly to *Laufkötter et al.*, 2013; *Marinov et al.*, 2013, Table 3], other studies have observed opposite trends in this region. For example, Steinberg et al. [2012] found a 61 % increase in mesozooplankton between 1994 and 2010 that coincided with an increase in picoplankton and a decline in diatoms (Lomas et al. 2010). While some of these differences could be explained by the difference in time periods, methodologies used and areas considered, the divergence of results suggest that further studies are needed to confirm these trends. In the North and Equatorial Indian basins, the two other regions with a significant decline in diatoms, nitrate declines significantly leading to a decline in both diatoms and chlorophytes. The percent declines are relatively large: ~4% y^{-1} reduction in nitrate corresponding with ~4% y^{-1} decline in diatoms and chlorophytes each (Table 2). These declines are matched by a concomitant increase in cyanobacteria (~9% y^{-1}increase). The result is a composition shift as cyanobacteria overtake chlorophytes as the dominant phytoplankton in the Equatorial Indian and are on the verge of overtaking them in the North Indian as the time series ended. The ability of cyanobacteria to survive in low nutrient conditions facilitates their advance over the more demanding nutrient requirements of the larger phytoplankton. Coccolithophores are efficient users of low nutrients as well, and their abundances increase significantly over vast areas of these basins (Figure 7). However, their abundances remain low

throughout the time series and they are not major contributors to the phytoplankton community despite their statistically positive trends.

The patterns of significantly declining nitrate and resultant declines in larger phytoplankton occur in the North Indian basin despite a significant increase in MLD, which is contrary to the physical-biological interactions observed elsewhere over this time period and with established paradigm. We suggest that despite the statistically significant deepening of the MLD in this region, the depth over which it increases (2 m in 15 years) may not have been large enough to reach nutrient-rich layers that could enrich the surface waters with nitrate and reverse the emerging and observed phytoplankton community shift observed here. We note however that this is a mean over a basin and therefore may obscure the magnitude of local regions that determine the mean. It is also possible that the use of annual means obscures seasonal trends in MLD in this monsoon-dominated system that are responsible for the nitrate decline and the resultant trends in phytoplankton.

A closer look at the spatial distribution of trends (Figure 2) indicates that the deepening of the MLD is mostly confined to the upwelling areas in the North and Equatorial Indian (along the western and northern coasts and off the southern tip of India). This MLD deepening is large compared to the background and corresponds with most of the decline in nutrients and phytoplankton in these basins. These relationships are consistent with upwelling regions, where MLD deepening is associated with nutrient declines, unlike the inverse relationship paradigm seen in other parts of the oceans. The relationships and observations here would suggest a reduction in upwelling. Note that while iron the North and Equatorial Indian increases significantly, this nutrient is most likely not limiting in these regions and therefore is not expected to impact phytoplankton concentration.

While the reasons for the existence of significant trends in only the northern latitudes of the Atlantic and Pacific Ocean remain unclear, one hypothesis is that it could be related to the strong asymmetry in the transient response of air temperature to increasing CO_2, with the Northern hemisphere warming up considerably faster than the Southern hemisphere [*Meehl et al.*, 2007]. This asymmetry has been largely attributed to the land-ocean differences between the hemispheres as well as the Arctic sea ice melt and the role of currents in 'distributing' this increase in temperature across the oceans. This hypothesis could explain the shallowing of the MLD north of 10°N that coincides with a decline in nutrient and phytoplankton while the southern hemisphere has few significant trends in the physical conditions, nutrients and phytoplankton community. Another hypothesis is that these trends may be directly related to larger climate oscillation such as the Pacific Decadal Oscillation (PDO) and the North Atlantic Oscillation (NAO). The PDO is a climate oscillation that is based on the variation of North Pacific sea surface temperature and in the twentieth century has had oscillations of ~20-30 years [*Mantua et al.*, 1997]. The cold phase refers to temperatures in the eastern Pacific. In late 1998, the PDO entered a cold phase that only lasted for four years and was followed by a warm phase that lasted for three years before switching again to a cold phase after 2008 [*Wu*, 2013]. The diatom declines reported here are mostly found in the western and central portions of the North Pacific, where MLD temperature increases, consistent with the patterns of the cold phase. There have been several reports that the PDO and NAO affect interannual variability in phytoplankton (using total chlorophyll) as well as the timing and magnitude of the blooms. *Chiba et al.* [2012] for example show that the PDO affects the timing of the bloom in the western North Pacific. In the North Atlantic, *Henson et al.* [2009] find a decadal-scale periodicity in the timing of the subpolar bloom that is correlated to the NAO. So although the length of the record used to detect trends here does not allow us to conclude whether these oscillations may be driving the trends

observed in this study, it is likely that these climate oscillations may play a role in the trends observed.

The existence of positive trends in only nutrients and PAR in the regions south of 10°N in the Atlantic and Pacific Ocean suggests that the increase in nutrients in those regions is not considerably affecting the phytoplankton composition. The only significant trend in phytoplankton is observed in the Equatorial Pacific for coccolithophores. A spatial representation of these trends (Figure 7) shows that this trend originates from the western Equatorial Pacific where coccolithophores are abundant in the model. Although it has been reported that coccolithophores are present in the western Equatorial Pacific [*Hagino et al.*, 2000; *Okada and Honjo*, 1973], other investigators [*DiTullio et al.*, 2003; *Ishizaka et al.*, 1997] report low to negligible relative abundance of coccolithophores in this area.

In the Southern Ocean, PAR, silicate and nitrate increase significantly. The increase in nutrients in this region could be attributed to the strengthening of the westerlies in this region [e.g. *Swart and Fyfe*, 2012]. An increase in the westerlies would in turn lead to a deepening of the MLD and therefore could drive the upward trend that we find in nutrients. The MLD in this region however is shallowing, not deepening. The pattern of trends in MLD in the Southern Ocean are highly heterogeneous and therefore although the trends based on spatially averaged MLD seem to be shallowing, a spatial representation of the trends in MLD (Figure 2**Figure**) clearly indicates some regions with considerable MLD deepening that could be related to intensified westerlies as suggested in previous modeling studies [*Marinov et al.*, 2013]. Similarly to our study, Alvain et al. [2013] also noted the existence of high spatial variability in diatom shifts between positive and negative Southern Annular Mode in the Southern Ocean. Soppa et al. [2014] also noted the high spatial variability in the trends of diatom abundance in the Southern Ocean. This heterogeneity in the trends in the Southern Ocean was also observed for Particulate Inorganic Carbon concentration

(PIC). Freeman & Lovenduski [2015] found that PIC concentration in the Southern Ocean declined by ~24% between 1998 and 2014. The difference between both studies could be explained by the difference in the definition of the Southern Ocean. Freeman & Lovenduski [2015] defined the Southern Ocean as south of 30°S whereas we define it as south of 45°S. Considering this and the spatial heterogeneity, as well as the fact that coccolithophores are not the only organisms producing PIC, it is not entirely surprising that we obtained different trends in this region.

The trends reported here represent an early attempt to improve our understanding of how phytoplankton composition and its drivers are changing. It is by no means intended to represent the effects of climate change since this would require a much longer time series than the 15 years investigated here [*Henson et al.*, 2010]. However, we believe it is important to monitor trends so we can assess shorter term emerging patterns. We acknowledge that the phytoplankton trends are derived from a model, and as such contain the uncertainties inherent in a model. We strive to overcome these drawbacks by using the best available data and methodologies, namely, satellite observations, in situ data, and data assimilation. The phytoplankton groups represented in the NOBM are meant to be representative of the end-to-end spectrum of functions of a phytoplankton community. The grouping of phytoplankton into functional groups are relevant to the biogeochemical community because they are the indicators of ecosystem dynamic and how they are changing. The phytoplankton composition from the model has been extensively validated and shown to adequately represent the spatial distribution of phytoplankton groups, but in the end the phytoplankton group distributions are more dependent upon model formulation than the total chlorophyll, which is corrected by satellite data assimilation. We use the information from the data assimilation to modify the phytoplankton responses, but these are indirect adjustments. While there is unfortunately, to this date, not enough in situ data on phytoplankton composition to confirm that

these trends do indeed exist, we believe that it is important to start with this type of investigation. The model used in this study could be improved by including additional functional groups (*Phaeocystis* spp., dinoflagellates, etc). Functional groups such as *Phaeocystis* spp. are in the process of being added and will improve the models representation of oceanic biogeochemistry. How the organization of the groups or lack of missing groups would affect the model depends on what groups are added, what the parameterizations are and how valid these parameterizations are. These models are, like nature, very complex (although less so than nature) and speculation about them is very difficult. However we speculate that the trends in the functional extremes, cyanobacteria and diatoms, observed in the current study would remain after we add additional intermediate phytoplankton groups such as *Phaeocystis* spp. The NOBM also lacks in its current representation of coastal waters which represent a limitation in the type of research that can be currently conducted. The multiplication of studies like these will allow the assessment of regions where common trends in phytoplankton composition are found and where discrepancies occur. The recent development of algorithms that allow the distinction of phytoplankton groups from satellite ocean color [e.g. *Alvain et al.*, 2008; *Hirata et al.*, 2011; *Sathyendranath et al.*, 2004] can contribute to this knowledge and can provide an interesting comparison to the approach used in our study. However, these algorithms also have uncertainties and limitations [*Rousseaux et al.*, 2013]. Our best hope for reducing the uncertainties in global ocean phytoplankton distributions can come from innovative new ocean color sensors, such as the Pre-Aerosol, Clouds, and ocean Ecosystems (PACE), which is designed to capture the variability of phytoplankton using hyper-spectral technology.

In conclusion, by assimilating the last 15 years of satellite ocean chlorophyll in an established biogeochemical model, we find that there are some significant changes in physical conditions, nutrients and phytoplankton communities in the high latitudes. In the Northern hemisphere, there is a

shallowing of the MLD and a decline in nutrients that affects differently the phytoplankton community depending on the regions. In the Southern Ocean, there is a significant increase in nutrients that does not seem to affect significantly the phytoplankton population. Some of the mechanisms driving these variations remain unknown but this provides an indication of the variability and the existence of trends during a 15 year long time series. While there is a clear need for in situ data on nutrients and phytoplankton communities to validate these results, this study provides some new information on the trends in phytoplankton composition at a global scale.

Acknowledgments

We thank the NASA Ocean Color project for providing the satellite chlorophyll data and the NASA Center for Climate Simulation for computational support. This paper was funded by the NASA MAP, and PACE Programs. Data used in this analysis can be obtained at the NASA GES-DISC Giovanni web location http://gdata1.sci.gsfc.nasa.gov/daac-bin/G3/gui.cgi?instance_id=ocean_model. We also thank the reviewers for their constructive feedback on this paper.

References

Agawin, N. S., C. M. Duarte, and S. Agusti (1998), Growth and abundance of Synechococcus sp. in a Mediterranean Bay: seasonality and relationship with temperature, *Marine Ecology Progress Series*, *170*, 45-53.

Agawin, N. S. R., C. M. Duarte, and S. Agusti (2000), Nutrient and Temperature Control of the Contribution of Picoplankton to Phytoplankton Biomass and Production, *Limnology and Oceanography*, *45*(3), 591-600.

Agirbas, E., V. Martinez-Vicente, R. J. Brewin, M.-F. Racault, R. Airs, and C. Llewellyn (2015), Temporal changes in total and size-fractioned chlorophyll-a in surface waters of three provinces in the Atlantic Ocean (September to November) between 2003 and 2010, *Journal of Marine Systems*.

Aiken, J., and A. Bale (2000), An introduction to the Atlantic Meridional Transect (AMT) programme, *Progress in Oceanography*, *45*(3), 251-256.

Alheit, J., and M. Niquen (2004), Regime shifts in the Humboldt Current ecosystem, *Progress in Oceanography*, *60*(2), 201-222.

Alvain, S., C. Moulin, Y. Dandonneau, and F. M. Bréon (2005), Remote sensing of phytoplankton groups in case 1 waters from global SeaWiFS imagery, *Deep-Sea Research Part I*, *52*(11), 1989-2004.

Alvain, S., C. Moulin, Y. Dandonneau, and H. Loisel (2008), Seasonal distribution and succession of dominant phytoplankton groups in the global ocean: A satellite view, *Global Biogeochemical Cycles*, *22*(3), GB3001, doi:3010.1029/2007GB003154.

Alvain, S., C. Le Quéré, L. Bopp, M.-F. Racault, G. Beaugrand, D. Dessailly, and E. T. Buitenhuis (2013), Rapid climatic driven shifts of diatoms at high latitudes, *Remote Sensing of Environment*, *132*, 195-201.

Antoine, D., A. Morel, H. R. Gordon, V. F. Banzon, and R. H. Evans (2005), Bridging ocean color observations of the 1980s and 2000s in search of long-term trends, *Journal of Geophysical Research: Oceans 110*(C6).

Barnard, R., S. Batten, G. Beaugrand, C. Buckland, D. Conway, M. Edwards, J. Finlayson, L. Gregory, N. Halliday, and A. John (2004), Continuous plankton records: Plankton atlas of the North Atlantic Ocean (1958-1999). II. Biogeographical charts, *Marine Ecology-progress Series*, S11-75.

Beaugrand, G. (2004), The North Sea regime shift: evidence, causes, mechanisms and consequences, *Progress in Oceanography*, *60*(2), 245-262.

Beaugrand, G., P. C. Reid, F. Ibanez, J. A. Lindley, and M. Edwards (2002), Reorganization of North Atlantic marine copepod biodiversity and climate, *Science*, *296*(5573), 1692-1694.

Beaulieu, C., S. A. Henson, J. L. Sarmiento, J. P. Dunne, S. C. Doney, R. Rykaczewski, and L. Bopp (2013), Factors challenging our ability to detect long-term trends in ocean chlorophyll.

Behrenfeld, M. J., R. T. O'Malley, D. A. Siegel, C. R. McClain, J. L. Sarmiento, G. C. Feldman, A. J. Milligan, P. G. Falkowski, R. M. Letelier, and E. S. Boss (2006), Climate-driven trends in contemporary ocean productivity, *Nature*, *444*(7120), 752-755.

Bopp, L., O. Aumont, P. Cadule, S. Alvain, and M. Gehlen (2005), Response of diatoms distribution to global warming and potential implications: A global model study, *Geophysical Research Letters*, *32*(19).

Box, G. E., G. M. Jenkins, and G. C. Reinsel (1994), Time Analysis, Forecasting and Control, edited, Prentice-Hall, Englewood Cliffs NJ.

Boyce, D. G., M. Dowd, M. R. Lewis, and B. Worm (2014), Estimating global chlorophyll changes over the past century, *Progress in Oceanography*, *122*, 163-173.

Boyd, P. W., and S. C. Doney (2002), Modelling regional responses by marine pelagic ecosystems to global climate change, *Geophysical Research Letters*, *29*(16), 53-51.

Chiba, S., S. Batten, K. Sasaoka, Y. Sasai, and H. Sugisaki (2012), Influence of the Pacific Decadal Oscillation on phytoplankton phenology and community structure in the western North Pacific, *Geophysical Research Letters*, *39*(15), L15603.

Ciotti, A. M., M. R. Lewis, and J. J. Cullen (2002), Assessment of the relationships between dominant cell size in natural phytoplankton communities and the spectral shape of the absorption coefficient, *Limnology and Oceanography*, *47*(2), 404-417.

Conkright, M., J. Antonov, O. Baranova, T. Boyer, H. Garcia, R. Gelfeld, D. Johnson, R. Locarnini, P. Murphy, and T. O'Brien (2002), World Ocean Database, 2001. Volume 1, Introduction.

DiTullio, G. R., M. E. Geesey, D. R. Jones, K. L. Daly, L. Campbell, and W. O. Smith (2003), Phytoplankton assemblage structure and primary productivity along 170 degrees W in the South Pacific Ocean, *Marine Ecology Progress Series*, *255*, 55-80.

Doney, S. C. (2006), Oceanography: Plankton in a warmer world, *Nature*, *444*(7120), 695-696.

Eppley, R. W. (1972), Temperature and phytoplankton growth in the sea, *Fishery bulletin 70*(4), 1063-1085.

Flato, G., and G. Boer (2001), Warming asymmetry in climate change simulations, *Geophysical Research Letters*, *28*(1), 195-198.

Freeman, N. M., and N. S. Lovenduski (2015), Decreased calcification in the Southern Ocean over the satellite record, *Geophysical Research Letters*, *42*(6), 1834-1840.

Gent, P. R., and G. Danabasoglu (2011), Response to increasing Southern Hemisphere winds in CCSM4, *Journal of Climate*, *24*(19), 4992-4998.

Gregg, W. W. (2008), Assimilation of SeaWiFS ocean chlorophyll data into a three-dimensional global ocean model, *Journal of Marine Systems*, *69*(3-4), 205-225.

Gregg, W. W., and M. E. Conkright (2002), Decadal changes in global ocean chlorophyll, *Geophysical Research Letters*, *29*(15), 20-21.

Gregg, W. W., and N. W. Casey (2007), Modeling coccolithophores in the global oceans, *Deep-Sea Research Part II*, *54*(5-7), 447-477.

Gregg, W. W., and N. W. Casey (2009), Skill assessment of a spectral ocean-atmosphere radiative model, *Journal of Marine Systems*, *76*(1-2), 49-63.

Gregg, W. W., and N. W. Casey (2010), Improving the consistency of ocean color data: A step toward climate data records, *Geophysical Research Letters*, *37*(4), L04605.

Gregg, W. W., and C. S. Rousseaux (2014), Decadal Trends in Global Pelagic Ocean Chlorophyll: A New Assessment Combining Multiple Satellites, In Situ Data, and Models, *Journal of Geophysical Research*, *doi: 10.1002/2014JC010158*.

Gregg, W. W., N. W. Casey, and C. R. McClain (2005), Recent trends in global ocean chlorophyll, *Geophysical Research Letters*, *32*, L03606.

Gregg, W. W., N. W. Casey, and C. S. Rousseaux (2013), Global Surface Ocean Carbon Estimates in a Model Forced by MERRA, *NASA Technical Report Series on Global Modeling and Data Assimilation, NASA TM-2013-104606, Vol. 31, 39 pp.*

Gregg, W. W., P. Ginoux, P. S. Schopf, and N. W. Casey (2003), Phytoplankton and iron: validation of a global three-dimensional ocean biogeochemical model, *Deep Sea Research Part II: Topical Studies in Oceanography*, *50*(22-26), 3143-3169.

Gregg, W. W., N. W. Casey, J. E. O'Reilly, and W. E. Esaias (2009), An empirical approach to ocean color data: Reducing bias and the need for post-launch radiometric re-calibration, *Remote Sensing of Environment*, *113*(8), 1598-1612.

Hagino, K., H. Okada, and H. Matsuoka (2000), Spatial dynamics of coccolithophore assemblages in the Equatorial Western-Central Pacific Ocean, *Marine Micropaleontology*, *39*(1-4), 53-72.

Hashioka, T., M. Vogt, Y. Yamanaka, C. Le Quéré, E. T. Buitenhuis, M. Aita, S. Alvain, L. Bopp, T. Hirata, and I. D. Lima (2013), Phytoplankton competition during the spring bloom in four plankton functional type models.

Hays, G. C., A. J. Richardson, and C. Robinson (2005), Climate change and marine plankton, *Trends in Ecology & Evolution*, *20*(6), 337-344.

Henson, S. A., J. P. Dunne, and J. L. Sarmiento (2009), Decadal variability in North Atlantic phytoplankton blooms, *Journal of Geophysical Research*, *114*(C4), C04013.

Henson, S. A., J. L. Sarmiento, J. P. Dunne, L. Bopp, I. D. Lima, S. C. Doney, J. John, and C. Beaulieu (2010), Detection of anthropogenic climate change in satellite records of ocean chlorophyll and productivity, *Biogeosciences*, *7*, 621-640.

Hinder, S. L., G. C. Hays, M. Edwards, E. C. Roberts, A. W. Walne, and M. B. Gravenor (2012), Changes in marine dinoflagellate and diatom abundance under climate change, *Nature Climate Change*, *2*(4), 271-275.

Hirata, T., N. J. Hardman-Mountford, R. J. W. Brewin, J. Aiken, R. Barlow, K. Suzuki, T. Isada, E. Howell, T. Hashioka, and M. Noguchi-Aita (2011), Synoptic relationships between surface Chlorophyll-a and diagnostic pigments specific to phytoplankton functional types, *Biogeosciences*, *8*, 311-327.

Ishizaka, J., K. Harada, K. Ishikawa, H. Kiyosawa, H. Furusawa, Y. Watanabe, H. Ishida, K. Suzuki, N. Handa, and M. Takahashi (1997), Size and taxonomic plankton community structure and carbon flow at the equator, 175°E during 1990-1994, *Deep Sea Research Part II: Topical Studies in Oceanography*, *44*(9-10), 1927-1949.

Laufkötter, C., M. Vogt, and N. Gruber (2013), Long-term trends in ocean plankton production and particle export between 1960–2006, *Biogeosciences*, *10*(11), 7373-7393.

Li, W. K. W. (1998), Annual average abundance of heterotrophic bacteria and Synechococcus in surface ocean waters, *Limnology and Oceanography*, *43*(7), 1746-1753.

Lomas, M. W., D. K. Steinberg, T. Dickey, C. A. Carlson, N. B. Nelson, R. H. Condon, and N. R. Bates (2010), Increased ocean carbon export in the Sargasso Sea linked to climate variability is countered by its enhanced mesopelagic attenuation, *Biogeosciences*, *7*(1), 57-70.

Mantua, N. J., S. R. Hare, Y. Zhang, J. M. Wallace, and R. C. Francis (1997), A Pacific interdecadal climate oscillation with impacts on salmon production, *Bulletin of the American Meteorological Society*, *78*(6), 1069-1079.

Marinov, I., S. C. Doney, I. D. Lima, K. Lindsay, J. K. Moore, and N. Mahowald (2013), North-South asymmetry in the modeled phytoplankton community response to climate change over the 21st century, *Global Biogeochemical Cycles*, *27*(4), 1274-1290.

Martinez, E., D. Antoine, F. D'Ortenzio, and B. Gentili (2009), Climate-driven basin-scale decadal oscillations of oceanic phytoplankton, *Science*, *326*(5957), 1253-1256.

Masotti, I., C. Moulin, S. Alvain, L. Bopp, A. Tagliabue, and D. Antoine (2011), Large-scale shifts in phytoplankton groups in the Equatorial Pacific during ENSO cycles, *Biogeosciences 8*(2), 539-550.

Meehl, G. A., T. F. Stocker, W. D. Collins, P. Friedlingstein, A. T. Gaye, J. M. Gregory, A. Kitoh, R. Knutti, J. M. Murphy, and A. Noda (2007), Global climate projections, *Climate change*, *3495*, 747-845.

Mouw, C. B., and J. A. Yoder (2006), Optical determination of phytoplankton size composition from global SeaWiFS imagery, *Journal of Geophysical Research*, *115*(C12), C12018.

Okada, H., and S. Honjo (1973), The distribution of oceanic coccolithophorids in the Pacific, *Deep-Sea Research*, *20*, 355-364.

Polovina, J. J., and P. A. Woodworth (2012), Declines in phytoplankton cell size in the subtropical oceans estimated from satellite remotely-sensed temperature and chlorophyll, 1998–2007, *Deep Sea Research Part II: Topical Studies in Oceanography*, *77*, 82-88.

Polovina, J. J., E. A. Howell, and M. Abecassis (2008), Ocean's least productive waters are expanding, *Geophysical Research Letters*, *35*(3), 1-5.

Racault, M.-F., C. Le Quéré, E. Buitenhuis, S. Sathyendranath, and T. Platt (2012), Phytoplankton phenology in the global ocean, *Ecological Indicators*, *14*(1), 152-163.

Richardson, A. J., and D. S. Schoeman (2004), Climate impact on plankton ecosystems in the Northeast Atlantic, *Science*, *305*(5690), 1609-1612.

Rienecker, M. M., M. J. Suarez, R. Gelaro, R. Todling, J. Bacmeister, E. Liu, M. G. Bosilovich, S. D. Schubert, L. Takacs, and G.-K. Kim (2011), MERRA: NASA''s Modern-Era Retrospective Analysis for Research and Applications, *Journal of Climate*, *24*(14).

Rousseaux, C., T. Hirata, and W. Gregg (2013), Satellite views of global phytoplankton community distributions using an empirical algorithm and a numerical model, *Biogeosciences Discussions*, *10*(1).

Rousseaux, C. S., and W. W. Gregg (2012), Climate variability and phytoplankton composition in the Pacific Ocean, *Journal of Geophysical Research*, *117*, C10006.

Sathyendranath, S., L. Watts, E. Devred, T. Platt, C. Caverhill, and H. Maass (2004), Discrimination of diatoms from other phytoplankton using ocean-colour data, *Marine Ecology Progress Series*, *272*, 59-68.

Soppa, M. A., T. Hirata, B. Silva, T. Dinter, I. Peeken, S. Wiegmann, and A. Bracher (2014), Global Retrieval of Diatom Abundance Based on Phytoplankton Pigments and Satellite Data, *Remote Sensing*, *6*(10), 10089-10106.

Steinacher, M., F. Joos, T. Frölicher, L. Bopp, P. Cadule, V. Cocco, S. Doney, M. Gehlen, K. Lindsay, and J. Moore (2010), Projected 21st century decrease in marine productivity: a multi-model analysis, *Biogeosciences*, *7*(3), 979-1005.

Steinberg, D. K., M. W. Lomas, and J. S. Cope (2012), Long-term increase in mesozooplankton biomass in the Sargasso Sea: Linkage to climate and implications for food web dynamics and biogeochemical cycling, *Global Biogeochemical Cycles*, *26*(1).

Stocker, T., D. Qin, G. Plattner, M. Tignor, S. Allen, J. Boschung, A. Nauels, Y. Xia, V. Bex, and P. Midgley (2013), IPCC, 2013: Climate Change 2013: The Physical Science Basis. Contribution of Working Group I to the Fifth Assessment Report of the Intergovernmental Panel on Climate Change, edited, Cambridge: Cambridge University Press.

Swart, N., and J. Fyfe (2012), Observed and simulated changes in the Southern Hemisphere surface westerly wind-stress, *Geophysical Research Letters*, *39*(16).

Treusch, A. H., E. Demir-Hilton, K. L. Vergin, A. Z. Worden, C. A. Carlson, M. G. Donatz, R. M. Burton, and S. J. Giovannoni (2012), Phytoplankton distribution patterns in the northwestern Sargasso Sea revealed by small subunit rRNA genes from plastids, *The ISME journal*, *6*(3), 481-492.

Uitz, J., H. Claustre, A. Morel, and S. B. Hooker (2006), Vertical distribution of phytoplankton communities in open ocean: An assessment based on surface chlorophyll, *Journal of Geophysical Research*, *111*, C08005.

Werdell, P. J., and S. W. Bailey (2005), An improved in-situ bio-optical data set for ocean color algorithm development and satellite data product validation, *Remote Sensing of Environment*, *98*(1), 122-140.

Wernand, M. R., H. J. van der Woerd, and W. W. Gieskes (2013), Trends in ocean colour and chlorophyll concentration from 1889 to 2000, worldwide, *Plos One*, *8*(6), e63766.

Wu, C.-R. (2013), Interannual modulation of the Pacific Decadal Oscillation (PDO) on the low-latitude western North Pacific, *Progress in Oceanography*, *110*, 49-58.

Tables

	k_n	k_{Si}	k_{Fe}
Diatoms	1.00	0.20	0.12
Chlorophytes	0.67		0.08
Cyanobacteria	0.45		0.08
Coccolithophores	0.50		0.08

Table 1: Half saturation constant for nitrogen (k_n) silicat (k_{Si}) and iron (k_{Fe}) used in the NOBM.

	MLD (m)	Temperature (°C)	PAR (moles quanta m^{-2} d^{-1})	Nitrate (µM)	Silicate(µM)	Iron(µM)	Diatoms (µg chl l^{-1})	Chlorophytes (µg chl l^{-1})	Cyanobacteria (µg chl l^{-1})	Coccolithophores (µg chl l^{-1})	Total chlorophyll (µg chl l^{-1})
Global	**-0.20**	0.01	**0.09**	**-0.38**	-0.11	0.01	**-1.22**	-	1.51	0.70	-0.27
North Atlantic	-0.19	0.04	**0.32**	**-0.88**	-0.15	**-1.79**	-0.93	**-9.70**	-	**5.96**	**-1.29**
North Pacific	**-1.00**	0.19	**0.21**	**-1.10**	**-1.79**	**-1.26**	**-1.00**	-	-	-	**-1.07**
North Central Atlantic	-0.26	0.02	0.08	**-3.09**	0.43	**-1.19**	-0.24	-	**-1.56**	**-2.06**	**-1.57**
North Central Pacific	**-0.43**	-0.03	**0.08**	**-2.70**	**-1.87**	0.20	0.70	-	**-0.72**	0.43	**-1.05**
North Indian	**0.50**	0.01	-0.07	**-2.87**	-1.07	**1.47**	**-5.89**	**-2.73**	**9.83**	-	**-2.41**
Equatorial Atlantic	0.01	0.00	0.06	1.14	**3.97**	0.72	0.96	-0.36	-2.09	-	-0.81
Equatorial Pacific	0.30	0.01	0.04	-2.83	-0.85	0.01	0.00	-	0.35	**4.72**	-0.21
Equatorial Indian	0.25	0.05	0.00	**-4.95**	-1.37	**1.10**	**-2.22**	**-6.02**	**2.64**	-	**-1.21**
South Atlantic	-0.11	0.03	**0.09**	-0.71	0.18	0.85	0.22	-7.34	0.75	1.83	-0.11
South Pacific	-0.02	-0.02	**0.09**	0.65	0.94	0.02	0.17	-	-0.11	1.67	0.18
South Indian	**-0.61**	0.05	**0.13**	-0.22	-0.65	0.18	-1.11	-	0.20	-1.78	**-1.10**
Southern Ocean	-0.16	0.05	**0.20**	**0.13**	**0.23**	0.55	0.23	-	-	-	0.18

Table 2: Percent change per year in the physical conditions, nutrients and phytoplankton composition in the 12 oceanographic regions and at the global scale. Bold and highlighted yellow indicates that the linear regression was significant ($p<0.05$) over the period 1998-2012. '-' indicates that the concentration for this group was smaller than 0.001 µg chl L^{-1} in this region. Note that the values are representative of the MLD, the first layer of the model.

	MLD (m)	Temperature (°C)	PAR (moles quanta m^{-2} d^{-1})	Nitrate (µM)	Silicate(µM)	Iron(µM)	Diatoms (µg chl l^{-1})	Chlorophytes (µg chl l^{-1})	Cyanobacteria (µg chl l^{-1})	Coccolithophores (µg chl l^{-1})	Total chlorophyll (µg chl l^{-1})
Global	**-1.76**	0.03	**0.46**	**-0.32**	-0.11	0.00	**-0.006**	0.000	0.001	0.000	-0.005
North Atlantic	-1.97	0.07	**0.84**	**-1.84**	-0.20	**-0.14**	-0.026	**-0.003**	0.000	**0.007**	**-0.054**
North Pacific	**-8.47**	0.25	**0.58**	**-2.69**	**-5.39**	**-0.07**	**-0.044**	-0.001	0.000	0.000	**-0.050**
North Central Atlantic	-1.51	0.09	0.44	**-0.22**	0.03	**-0.18**	0.000	0.000	**-0.010**	**-0.002**	**-0.020**
North Central Pacific	**-2.84**	-0.11	**0.47**	**-0.23**	**-0.32**	0.01	0.000	0.000	**-0.003**	0.000	**-0.009**
North Indian	**2.01**	0.06	-0.45	**-2.46**	-0.45	**0.31**	**-0.007**	**-0.033**	**0.034**	0.000	**-0.076**
Equatorial Atlantic	0.02	-0.01	0.36	0.65	**0.92**	0.09	0.002	-0.003	-0.007	0.000	-0.022
Equatorial Pacific	1.35	0.04	0.29	-1.11	-0.36	0.00	0.000	-0.002	0.002	**0.016**	-0.004
Equatorial Indian	0.96	0.20	0.03	**-0.83**	-0.18	**0.11**	**-0.003**	**-0.031**	**0.020**	0.004	**-0.021**
South Atlantic	-0.74	0.09	**0.50**	-0.24	0.05	0.03	0.000	-0.005	0.003	0.001	-0.001
South Pacific	-0.15	-0.07	**0.48**	0.10	0.17	0.00	0.000	0.000	0.000	0.001	0.002
South Indian	**-4.85**	0.15	**0.72**	-0.03	-0.13	0.01	-0.002	-0.002	0.001	-0.003	**-0.015**
Southern Ocean	-2.79	0.04	**0.50**	**0.30**	**0.65**	0.02	0.005	0.000	0.000	0.000	0.004

Table 3: Linear difference between 2012 and 1998 in the physical conditions, nutrients and phytoplankton composition in the 12 oceanographic regions and at the global scale. Bold and highlighted yellow indicates that the linear regression was significant ($p<0.05$) over the period 1998-2012. Note that the values are representative of the MLD, the first layer of the model.

Study	Phytoplankton composition and/or size?	Time period	Method to determine phytoplankton composition	Area	Main finding on trends in phytoplankton composition
In Situ					
Agirbas et al. (2015)	Size	2003-2010 (Sep-Nov)	HPLC from AMT	Atlantic Ocean	Decline in microphytoplankton and increase in nano- and picoplankton in the North and Equatorial Atlantic. Increase in picoplankton in South Atlantic.
Corno et al. (2007)	Composition	1997-2004	HPLC/Flow cytometry	North Pacific Subtropical Gyre (HOT)	Decline in Prochlorococcus spp. Increase in picoeukaryotes and prymnesiophytes Shift in plankton assemblage composition
Hinder et al. (2012)	Composition	1960-2009	Continuous Plankton Recorder	Northeast Atlantic and North Sea	Decline in dinoflagellates and increase in some diatom species
Lomas et al. (2010)	Composition	1990-2007 (Jan-Apr)	HPLC and flow cytometry from BATS	North Atlantic subtropical gyre (BATS)	Increase in cyanobacteria by 64% Decline in diatoms by 110%
Montes Hugo et al. (2009)	Size and composition	1993-2006	HPLC and remote sensing	Western Antarctic Peninsula	Shifts in community composition with a greater (lesser) fraction of diatoms and large cells in the southern (northern) region. Note that size was determined from remote sensing and composition from HPLC
Remote Sensing					
Polovina and Woodworth (2012)	Size	1998-2007	SeaWiFS	Subtropic regions (30°S-30°N)	Decline in size by 2-4% (North Pacific, South Pacific and North Atlantic).
Freeman & Lovenduski (2015)	PIC (proxy for coccolithophores)	1998-2014	SeaWiFS and MODIS-Aqua	Southern Ocean	Decline in PIC by ~24%
Racault et al. (2014)	Size	2003-2010	SeaWIFS	Atlantic Ocean	Decline in microphytoplankton and increase in pico- and nano-phytoplankton in the North, Equatorial and South Atlantic
Model Simulations					
Marinov et al. (2013)	Composition and size	1880-2090	Model simulation	Global	Climate response differs fundamentally in the Northern

					and Southern Hemispheres. Decline in diatoms and small phytoplankton in the Northern Hemisphere and an increase in diatoms and decrease in small phytoplankton in the Southern Hemisphere
Laufkotter et al. (2013)	Composition and size	1960-2006	Model simulation	Global	Decline in small phytoplankton by 8.5% Decline in diatoms by 3%
Boyd and Doney (2002)	Composition	2060-2070	Model simulation	Global	Suggest future increase in nitrogen fixation in subtropical regions
Bopp et al. (2005)	Composition	140 years run	Model simulation	Global	Increase in small phytoplankton Decline in diatoms
Polovina et al. (2011)	Size	2000-2100	Model simulation	Global	Decline in large phytoplankton by 27% (North Pacific)

Table 4: Recent examples of relevant studies on trends in phytoplankton (composition or size) from in situ, remote sensing and modeling approaches.

Figures

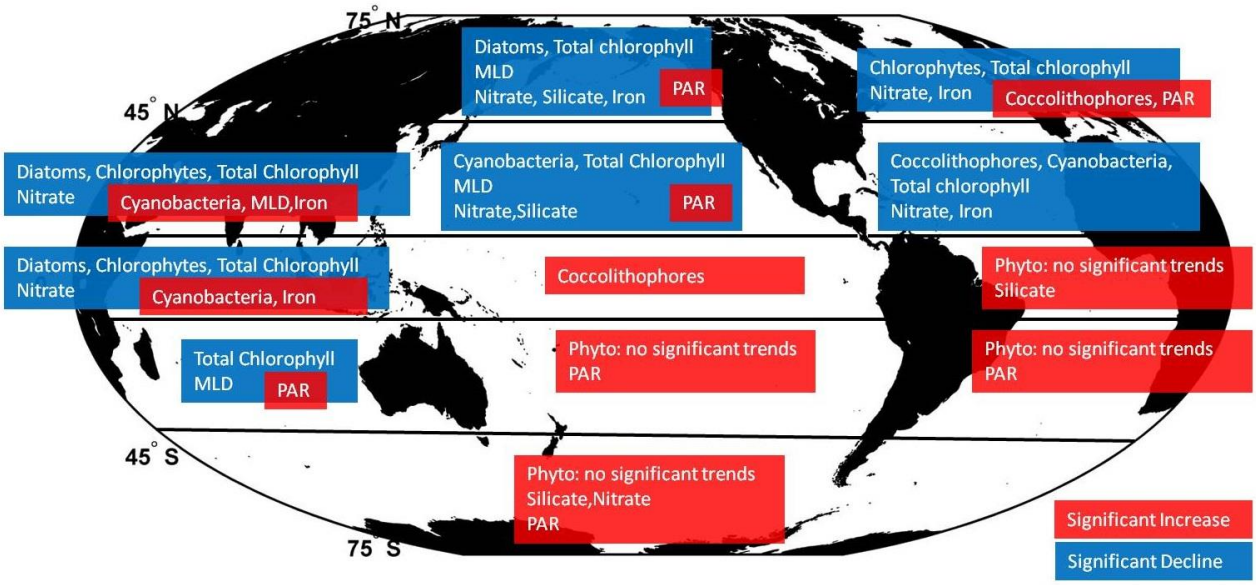

Figure 1: Significant increasing (red) or decreasing (blue) trends for each of the 12 oceanographic regions analyzed for the period from 1998 until 2012.

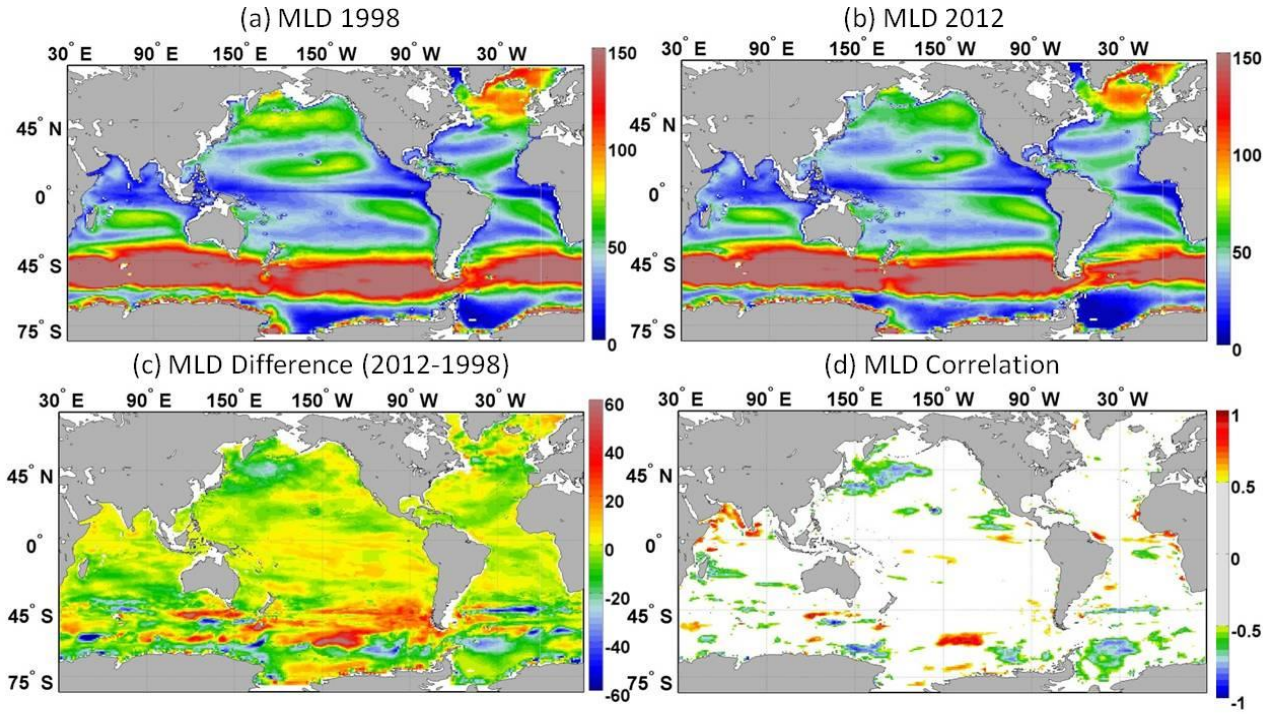

Figure 2: Global annual mean (best fit or trend line) MLD (m) in (a) 1998 and (b) 2012. (c) Difference between 2012 and 1998 and (d) correlation map showing locations where significant ($p<0.05$) trends were observed.

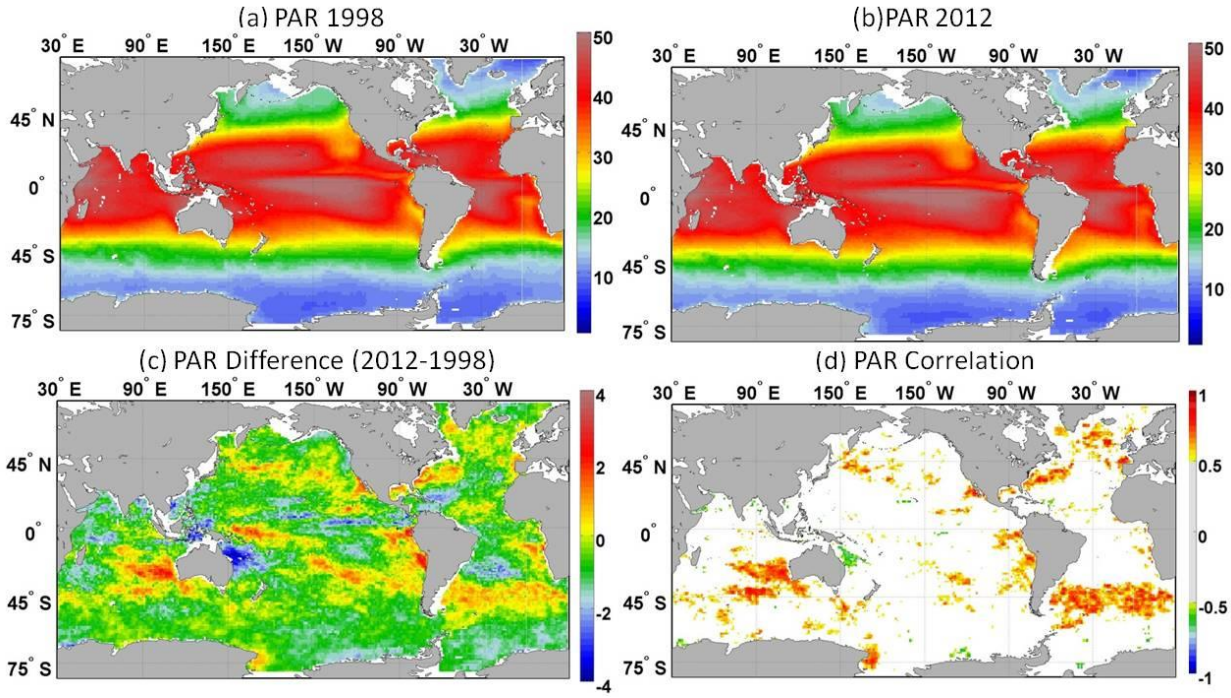

Figure 3: Global annual mean (best fit) PAR (moles quanta m^{-2} d^{-1}) in (a) 1998 and (b) 2012. (c) Difference between 2012 and 1998 and (d) correlation map showing locations where significant ($p<0.05$) trends were observed.

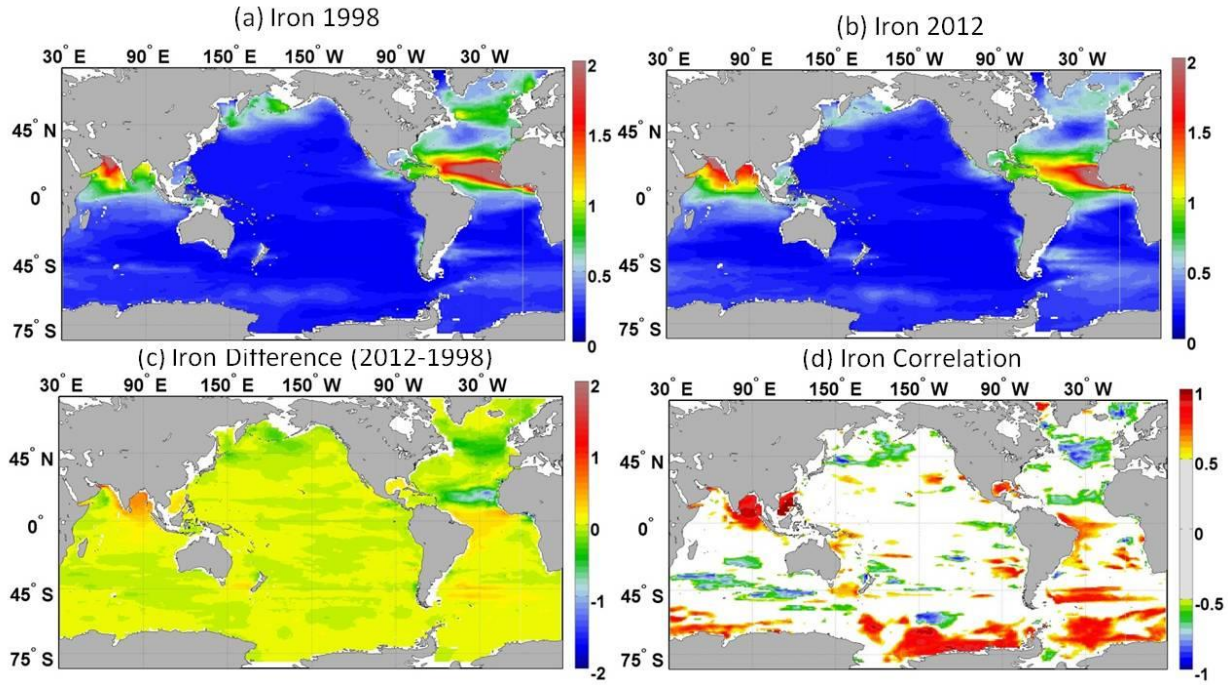

Figure 4: Global annual mean (best fit) iron concentration (µM) in (a) 1998 and (b) 2012. (c) Difference in concentrations between 2012 and 1998 and (d) correlation map showing locations where significant ($p<0.05$) trends were observed.

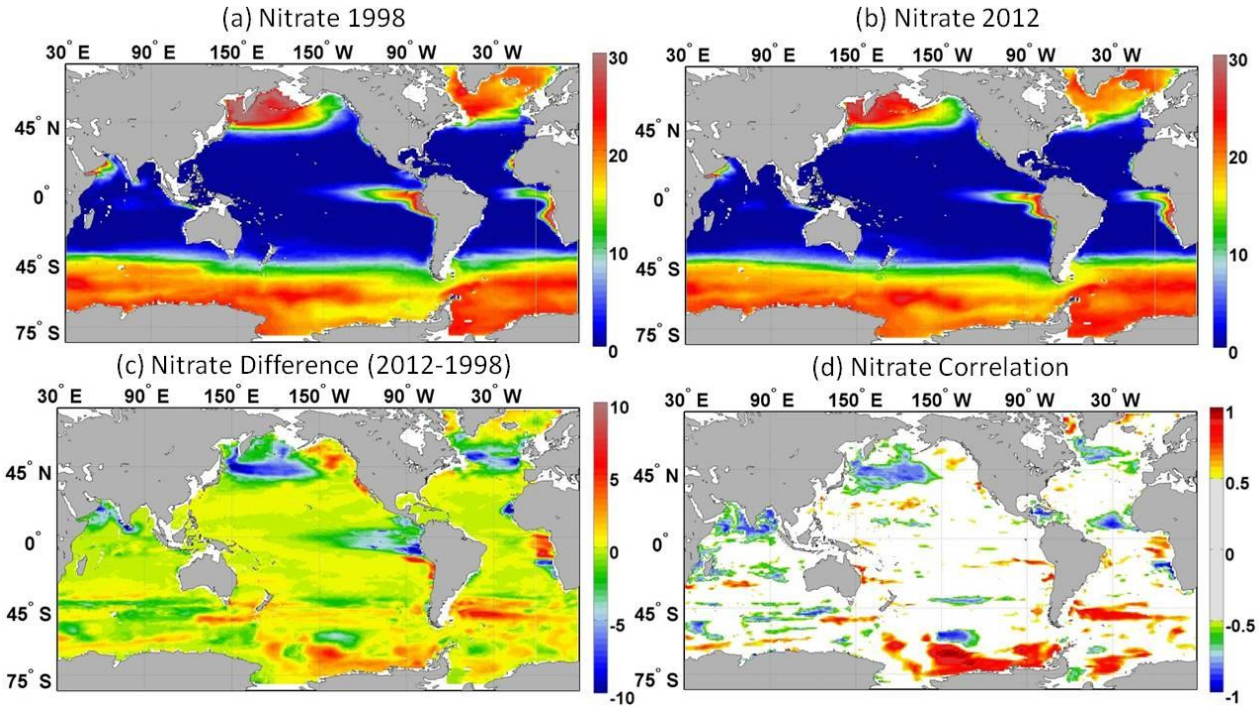

Figure 5: Global annual mean (best fit) nitrate concentration (µM) in (a) 1998 and (b) 2012. (c) Difference in concentrations between 2012 and 1998 and (d) correlation map showing locations where significant ($p<0.05$) trends were observed.

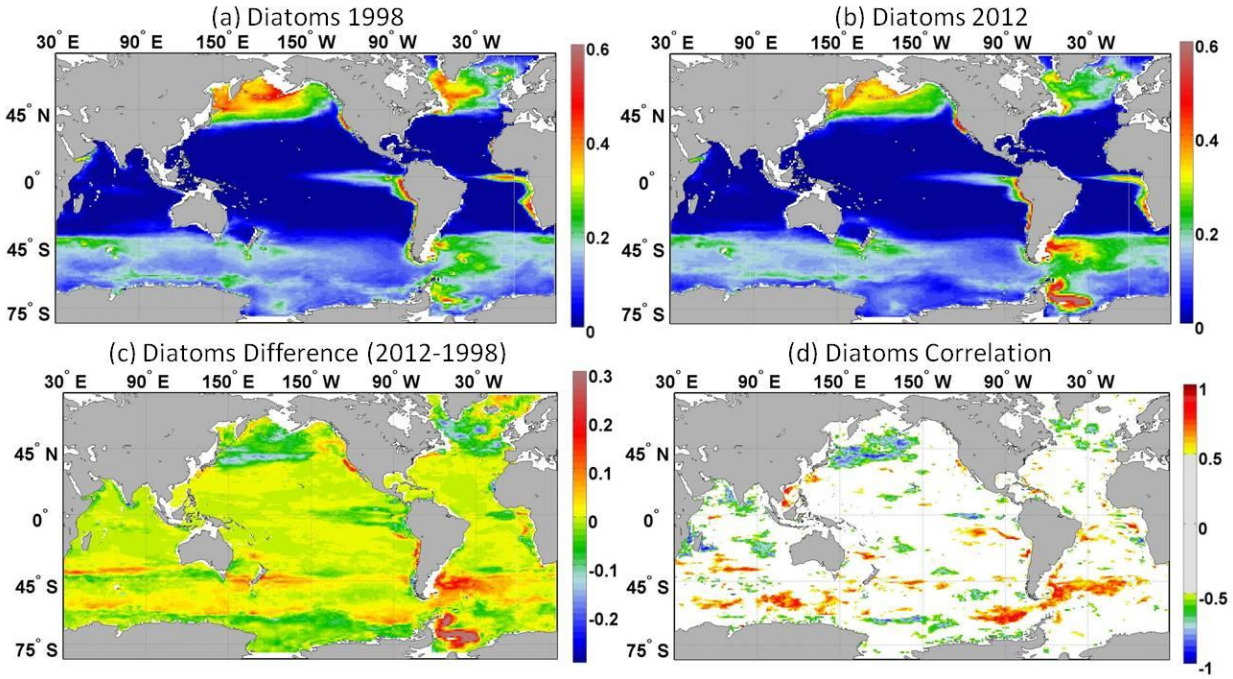

Figure 6: Global annual median (best fit) diatom concentration (µg chl l^{-1}) in (a) 1998 and (b) 2012. (c) Difference in concentrations between 2012 and 1998 and (d) correlation map showing locations where significant ($p<0.05$) trends were observed.

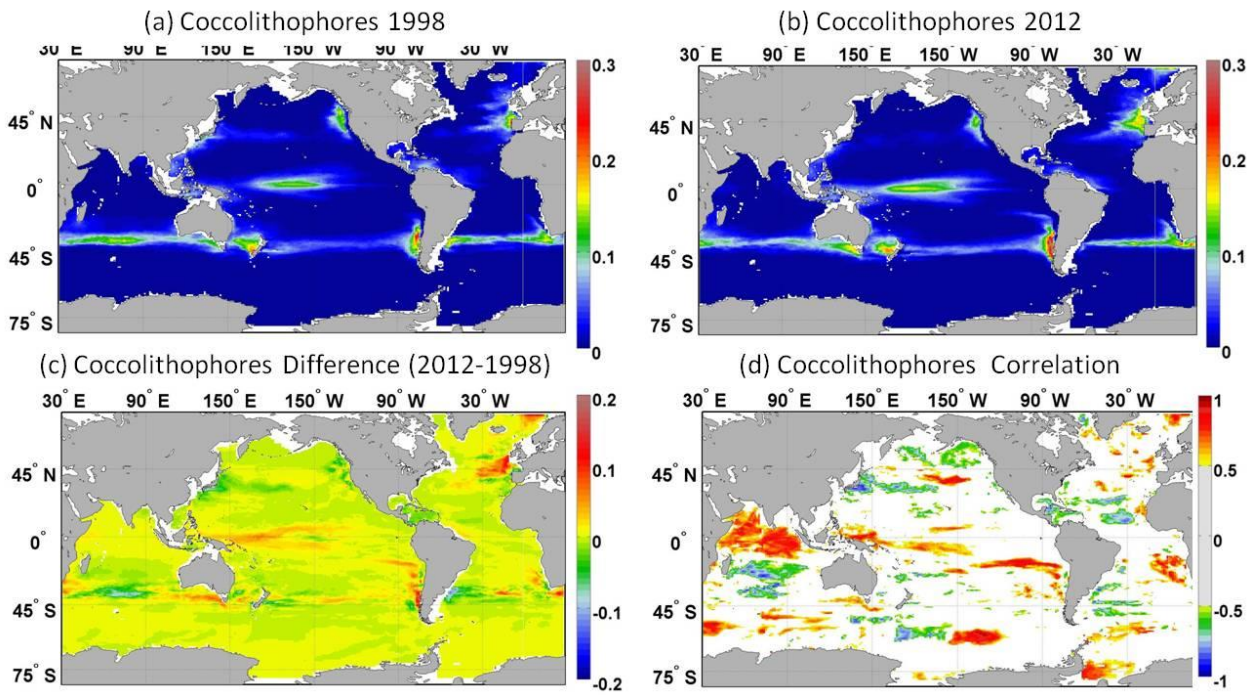

Figure 7: Global annual median (best fit) coccolithophores concentration (µg chl l^{-1}) in (a) 1998 and (b) 2012. (c) Difference in concentrations between 2012 and 1998 and (d) correlation map showing locations where significant ($p<0.05$) trends were observed.

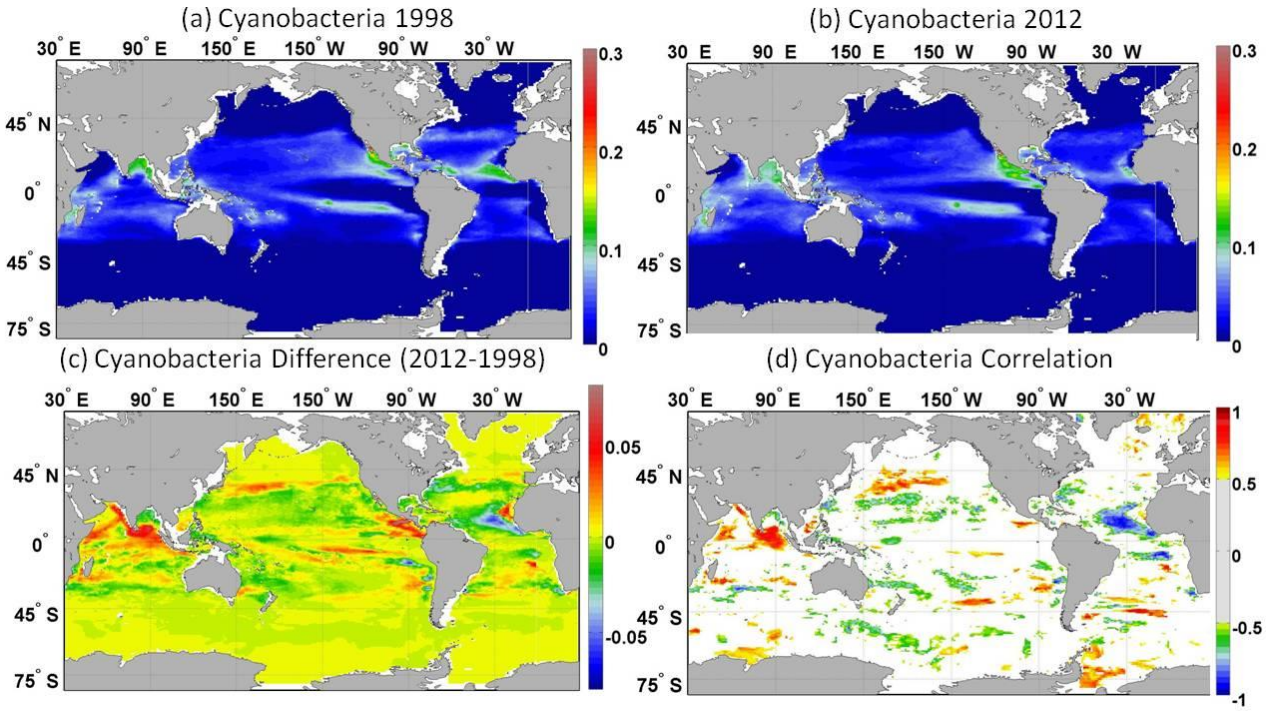

Figure 8: Global annual median (best fit) cyanobacteria concentration (µg chl l^{-1}) in (a) 1998 and (b) 2012. (c) Difference in concentrations between 2012 and 1998 and (d) correlation map showing locations where significant ($p<0.05$) trends were observed.

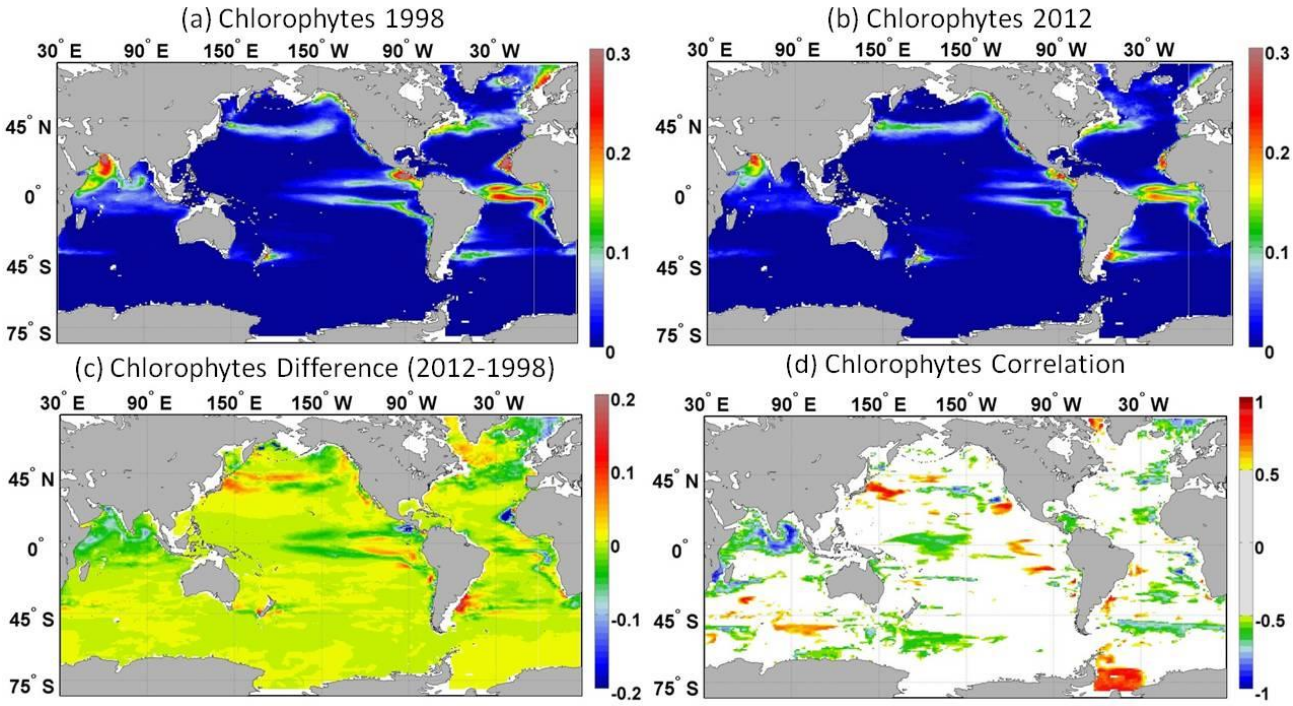

Figure 9: Global annual median (best fit) chlorophyte concentration (µg chl l^{-1}) in (a) 1998 and (b) 2012. (c) Difference in concentrations between 2012 and 1998 and (d) correlation map showing locations where significant ($p<0.05$) trends were observed.

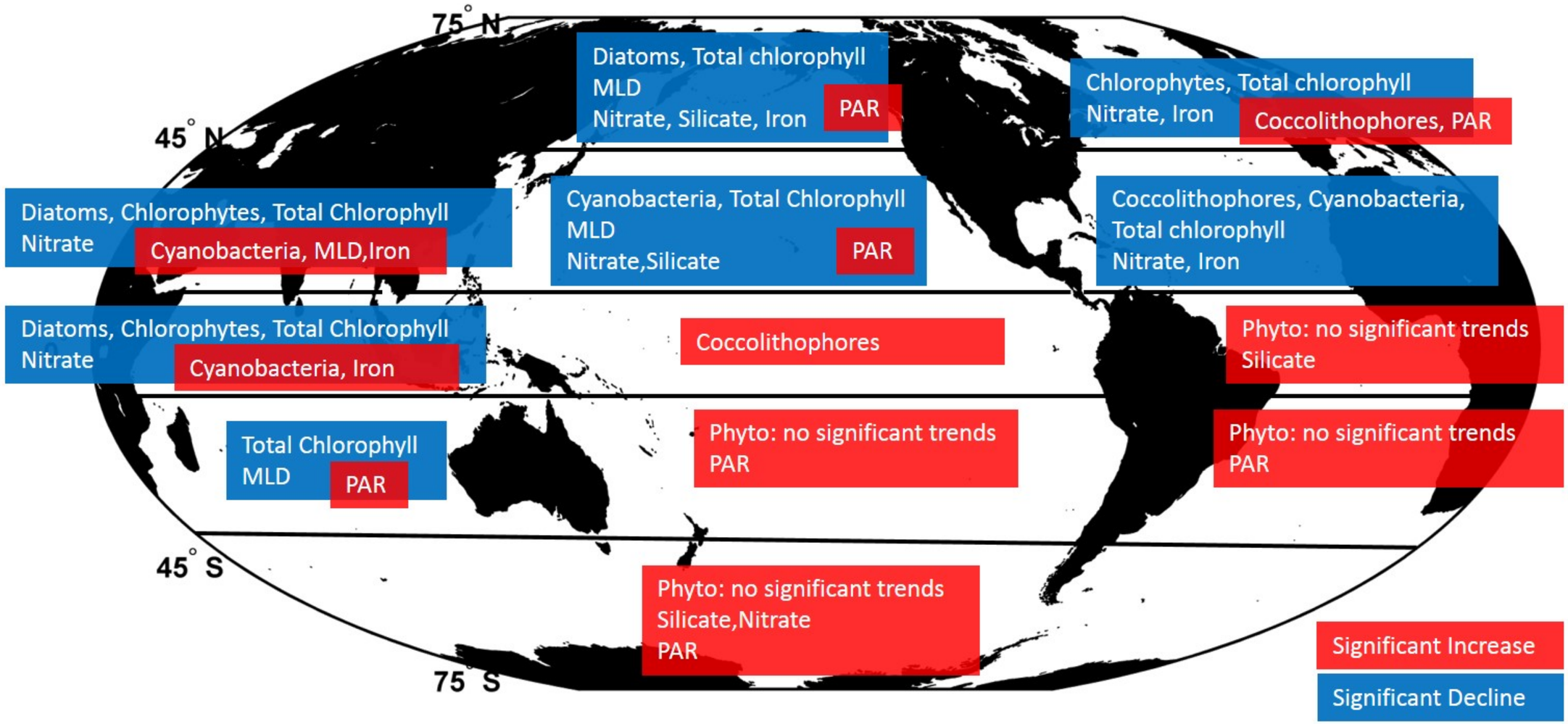
75° N
45° N
45° S
75° S
Diatoms, Total chlorophyll
MLD
Nitrate, Silicate, Iron
PAR
Chlorophytes, Total chlorophyll
Nitrate, Iron
Coccolithophores, PAR
Diatoms, Chlorophytes, Total Chlorophyll
Nitrate
Cyanobacteria, MLD,Iron
Cyanobacteria, Total Chlorophyll
MLD
Nitrate,Silicate
PAR
Coccolithophores, Cyanobacteria,
Total chlorophyll
Nitrate, Iron
Diatoms, Chlorophytes, Total Chlorophyll
Nitrate
Cyanobacteria, Iron
Coccolithophores
Phyto: no significant trends
Silicate
Total Chlorophyll
MLD
PAR
Phyto: no significant trends
PAR
Phyto: no significant trends
PAR
Phyto: no significant trends
Silicate,Nitrate
PAR
Significant Increase
Significant Decline

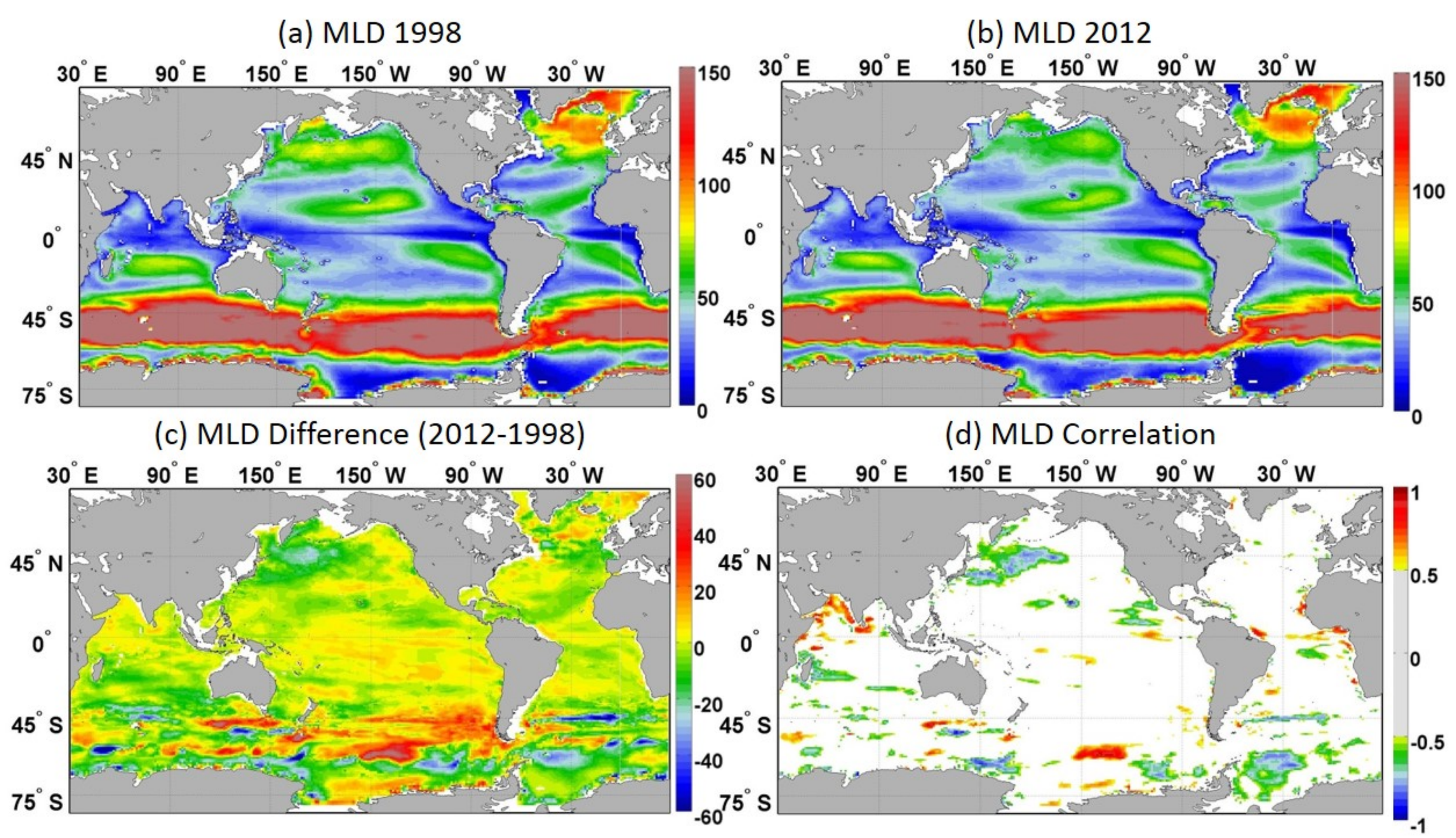
(a) MLD 1998
(b) MLD 2012
(c) MLD Difference (2012-1998)
(d) MLD Correlation
30° E
90° E
150° E
150° W
90° W
30° W
45° N
0°
45° S
75° S
150
100
50
0
60
40
20
0
-20
-40
-60
1
0.5
0
-0.5
-1

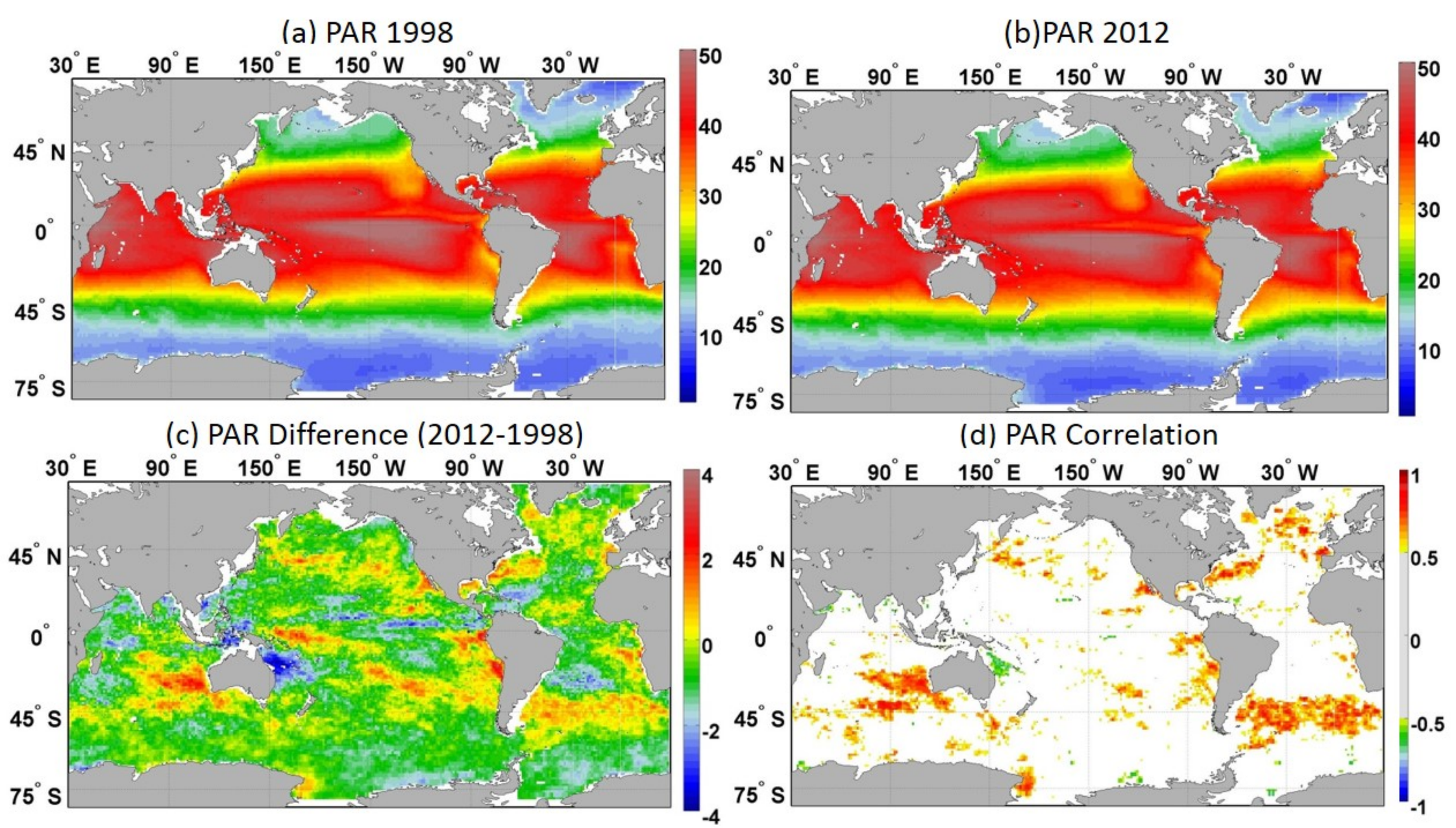
(a) PAR 1998
(b)PAR 2012
(c) PAR Difference (2012-1998)
(d) PAR Correlation
30° E
90° E
150° E
150° W
90° W
30° W
45° N
0°
45° S
75° S
50
40
30
20
10
4
2
0
-2
-4
1
0.5
0
-0.5
-1

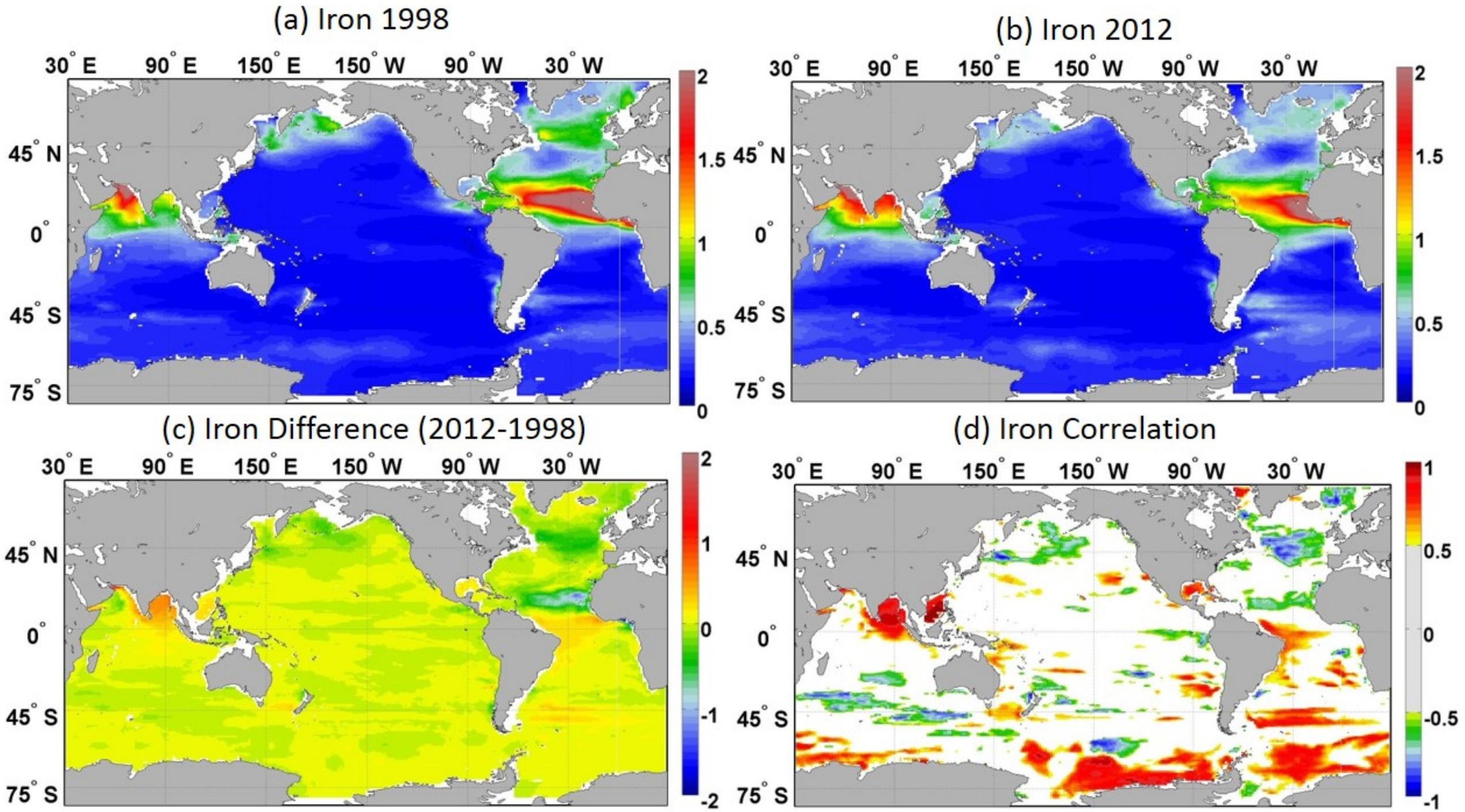
(a) Iron 1998
(b) Iron 2012
(c) Iron Difference (2012-1998)
(d) Iron Correlation
30° E
90° E
150° E
150° W
90° W
30° W
45° N
0°
45° S
75° S
2
1.5
1
0.5
0
-1
-2
-0.5

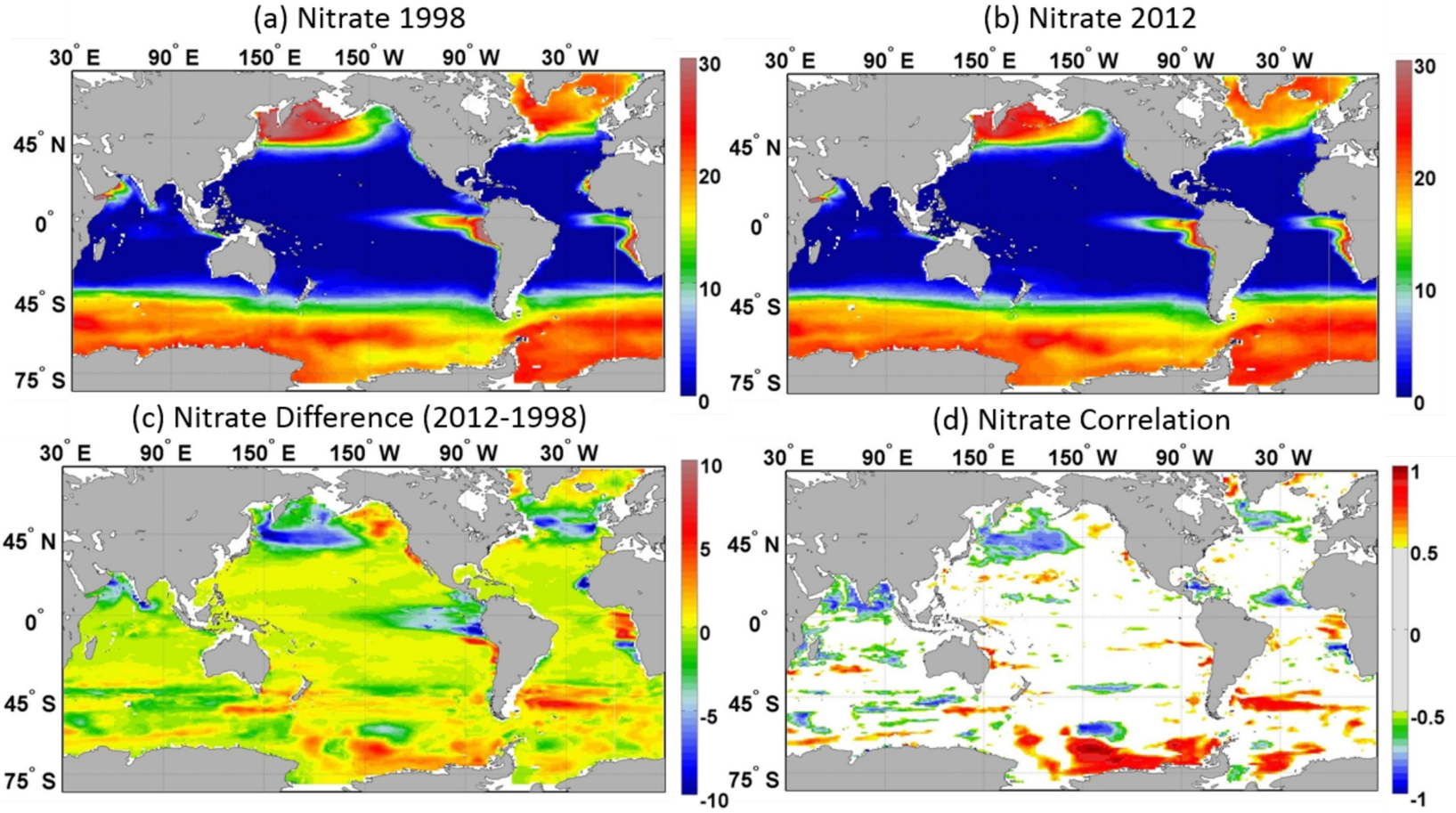
(a) Nitrate 1998
(b) Nitrate 2012
(c) Nitrate Difference (2012-1998)
(d) Nitrate Correlation
30° E
90° E
150° E
150° W
90° W
30° W
45° N
0°
45° S
75° S
30
20
10
0
10
5
0
-5
-10
1
0.5
0
-0.5
-1

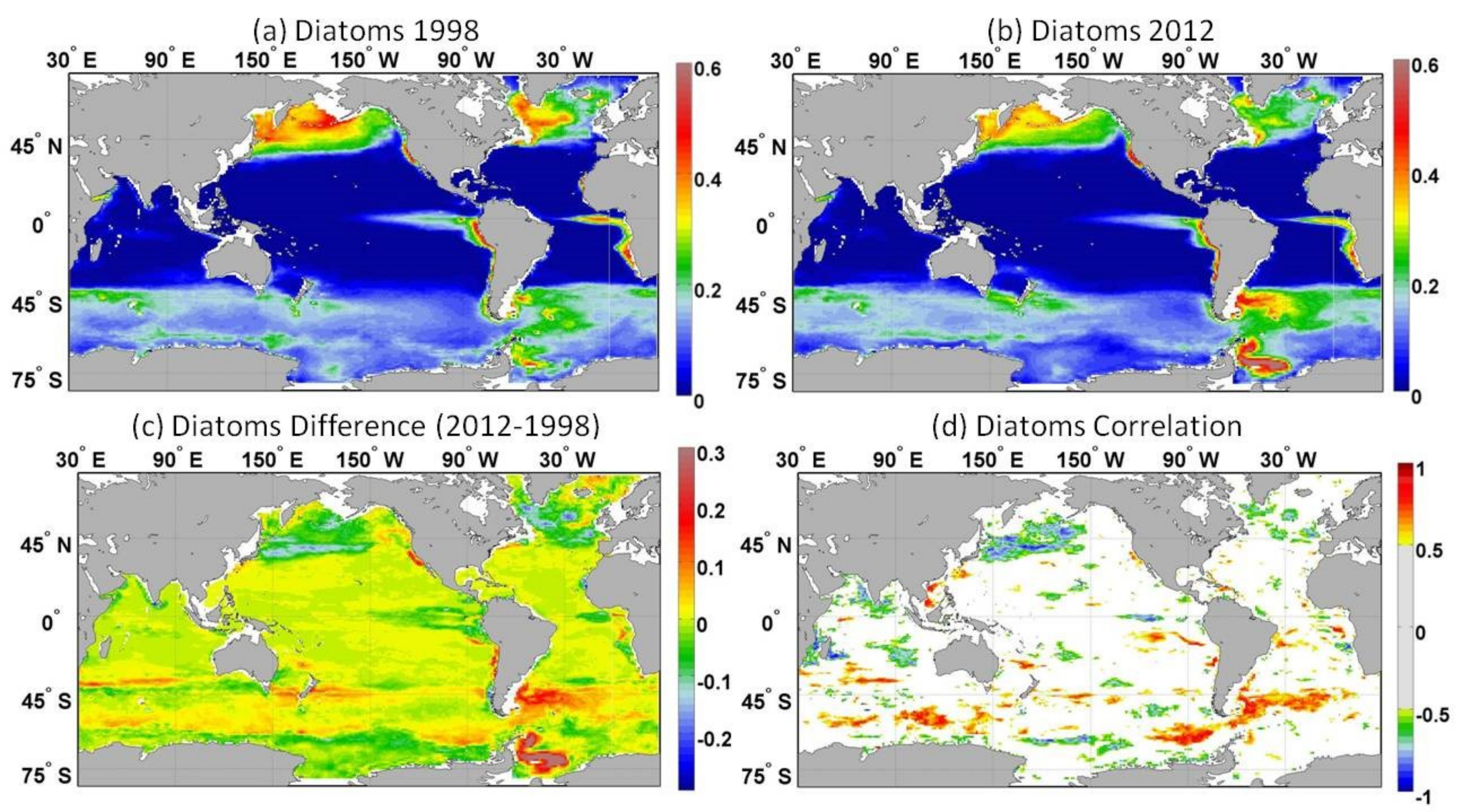
(a) Diatoms 1998
(b) Diatoms 2012
(c) Diatoms Difference (2012-1998)
(d) Diatoms Correlation
30° E
90° E
150° E
150° W
90° W
30° W
45° N
0°
45° S
75° S
0.6
0.4
0.2
0
0.3
0.2
0.1
0
-0.1
-0.2
1
0.5
0
-0.5
-1

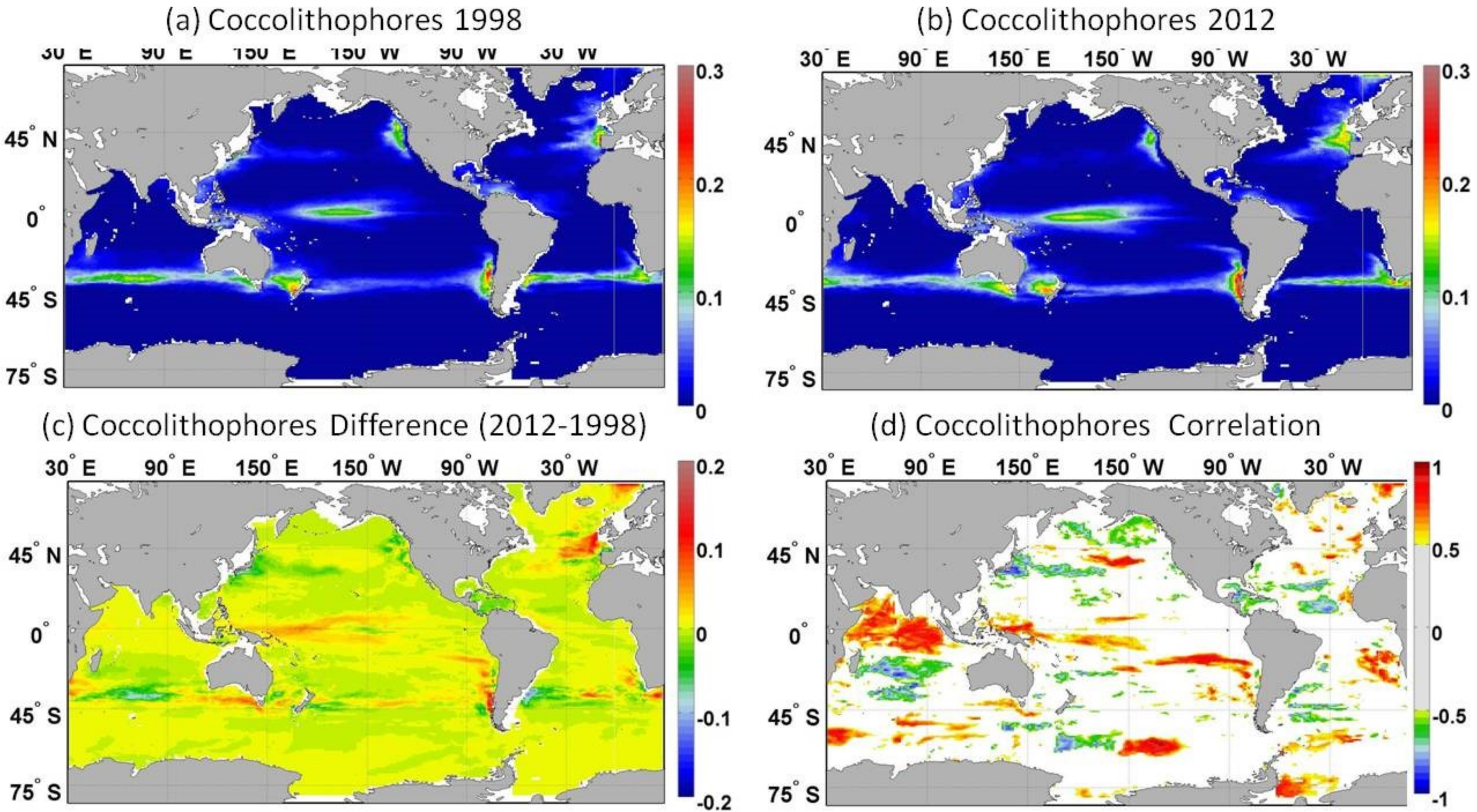
(a) Coccolithophores 1998
(b) Coccolithophores 2012
(c) Coccolithophores Difference (2012-1998)
(d) Coccolithophores Correlation
30° E
90° E
150° E
150° W
90° W
30° W
45° N
0°
45° S
75° S
0.3
0.2
0.1
0
-0.2
-0.1
1
0.5
-0.5
-1

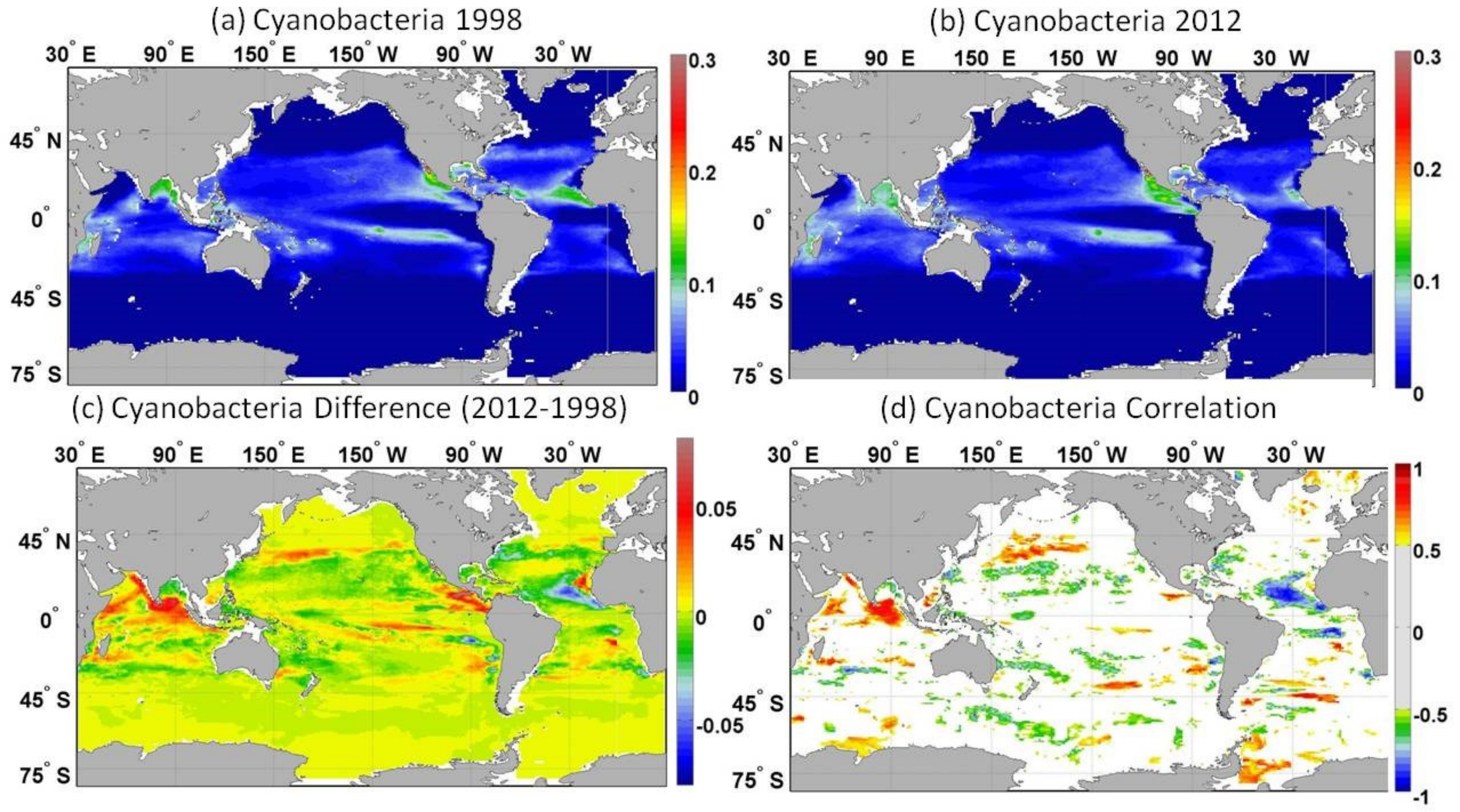
(a) Cyanobacteria 1998
(b) Cyanobacteria 2012
(c) Cyanobacteria Difference (2012-1998)
(d) Cyanobacteria Correlation
30° E
90° E
150° E
150° W
90° W
30° W
45° N
0°
45° S
75° S
0.3
0.2
0.1
0
0.05
-0.05
1
0.5
-0.5
-1

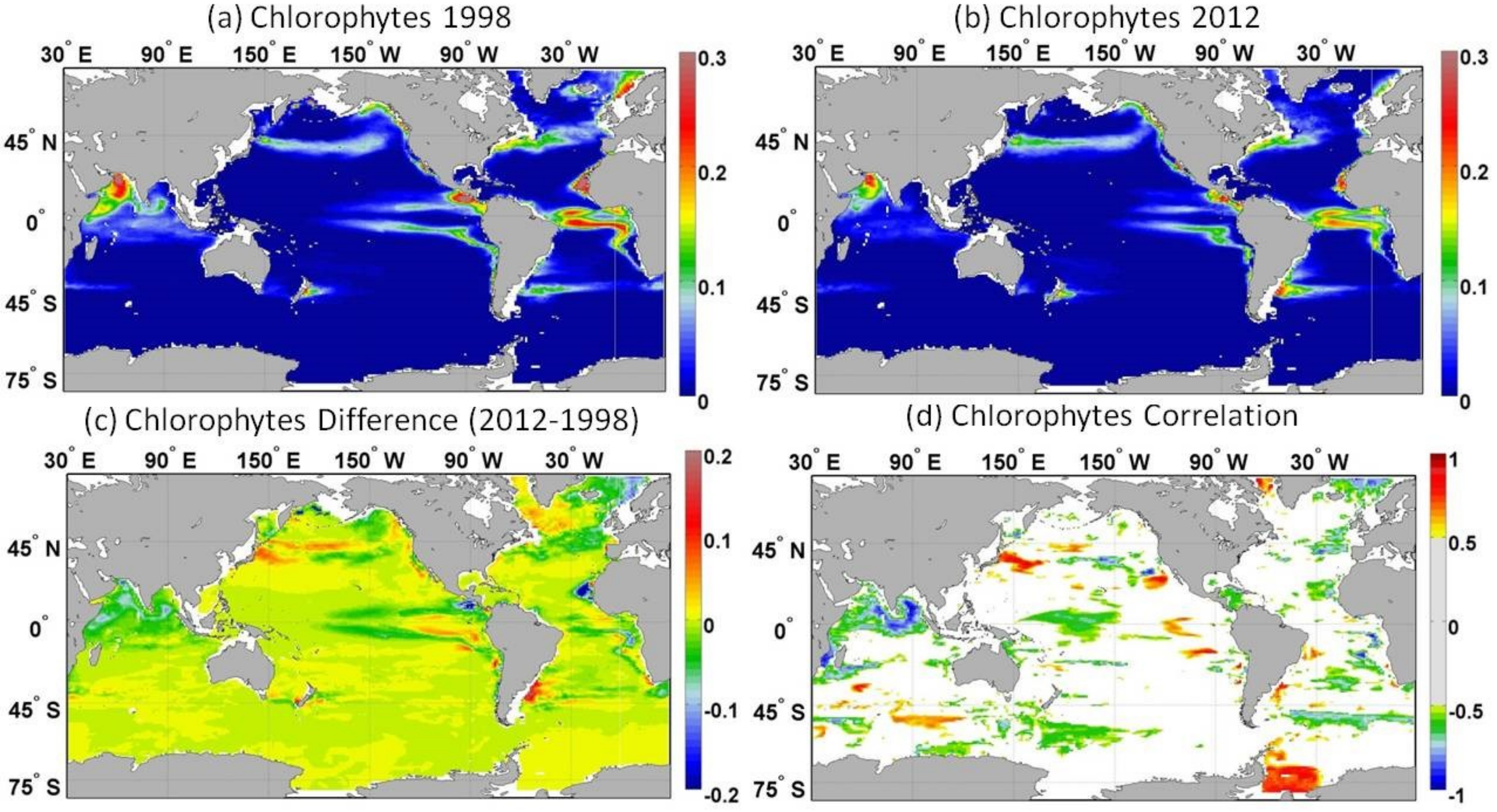
(a) Chlorophytes 1998
(b) Chlorophytes 2012
(c) Chlorophytes Difference (2012-1998)
(d) Chlorophytes Correlation
30° E
90° E
150° E
150° W
90° W
30° W
45° N
0°
45° S
75° S
0.3
0.2
0.1
0
0.2
0.1
0
-0.1
-0.2
1
0.5
0
-0.5
-1